Northumbria Research Link

Citation: Naikoo, Gowhar A., Arshad, Fareeha, Almas, Muniba, Hassan, Israr U., Pedram, Mona Z., Aljabali, Alaa A.A., Mishra, Vijay, Serrano-Aroca, Ángel, Birkett, Martin, Charbe, Nitin B., Goyal, Rohit, Negi, Poonam, El-Tanani, Mohamed and Tambuwala, Murtaza M. (2022) 2D materials, synthesis, characterization and toxicity: A critical review. Chemico-Biological Interactions, 365. p. 110081. ISSN 0009-2797

Published by: Elsevier

URL: https://doi.org/10.1016/j.cbi.2022.110081 <https://doi.org/10.1016/j.cbi.2022.110081>

This version was downloaded from Northumbria Research Link: https://nrl.northumbria.ac.uk/id/eprint/49825/

Northumbria University has developed Northumbria Research Link (NRL) to enable users to access the University's research output. Copyright © and moral rights for items on NRL are retained by the individual author(s) and/or other copyright owners. Single copies of full items can be reproduced, displayed or performed, and given to third parties in any format or medium for personal research or study, educational, or not-for-profit purposes without prior permission or charge, provided the authors, title and full bibliographic details are given, as well as a hyperlink and/or URL to the original metadata page. The content must not be changed in any way. Full items must not be sold commercially in any format or medium without formal permission of the copyright holder. The full policy is available online: http://nrl.northumbria.ac.uk/policies.html

This document may differ from the final, published version of the research and has been made available online in accordance with publisher policies. To read and/or cite from the published version of the research, please visit the publisher's website (a subscription may be required.)

Northumbria University NEWCASTLE

University Library

Journal Pre-proof

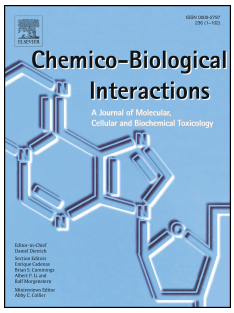

2D materials, synthesis, characterization and toxicity: A critical review

Gowhar A. Naikoo, Fareeha Arshad, Muniba Almas, Israr U. Hassan, Mona Z. Pedram, Alaa A.A. Aljabali, Vijay Mishra, Ángel Serrano-Aroca, Martin Birkett, Nitin B. Charbe, Rohit Goyal, Poonam Negi, Mohamed El-Tanani, Murtaza M. Tambuwala

PII: S0009-2797(22)00286-1

DOI: https://doi.org/10.1016/j.cbi.2022.110081

Reference: CBI 110081

To appear in: *Chemico-Biological Interactions*

Received Date: 14 March 2022

Revised Date: 21 July 2022

Accepted Date: 27 July 2022

Please cite this article as: G.A. Naikoo, F. Arshad, M. Almas, I.U. Hassan, M.Z. Pedram, A.A.A. Aljabali, V. Mishra, Á. Serrano-Aroca, M. Birkett, N.B. Charbe, R. Goyal, P. Negi, M. El-Tanani, M.M. Tambuwala, 2D materials, synthesis, characterization and toxicity: A critical review, *Chemico-Biological Interactions* (2022), doi: https://doi.org/10.1016/j.cbi.2022.110081.

This is a PDF file of an article that has undergone enhancements after acceptance, such as the addition of a cover page and metadata, and formatting for readability, but it is not yet the definitive version of record. This version will undergo additional copyediting, typesetting and review before it is published in its final form, but we are providing this version to give early visibility of the article. Please note that, during the production process, errors may be discovered which could affect the content, and all legal disclaimers that apply to the journal pertain.

© 2022 Published by Elsevier B.V.

Journal Pre-proof

2D materials, Synthesis, Characterization and Toxicity: A Critical Review

Gowhar A. Naikoo[1]*, Fareeha Arshad[2], Muniba Almas[3], Israr U. Hassan*[4], Mona Z. Pedram[5], Alaa A A Aljabali[6], Vijay Mishra[7], Ángel Serrano-Aroca[8], Martin Birkett[9], Nitin B Charbe[10], Rohit Goyal[11], Poonam Negi[11] Mohamed El-Tanani[12] and Murtaza M. Tambuwala[13]*

[1]Department of Mathematics and Sciences, College of Arts and Applied Sciences, Dhofar University, Salalah, Sultanate of Oman
[2]Department of Biochemistry, Aligarh Muslim University, U. P. India
[3]Department of Chemistry, The University of Poonch Rawalakot, Azad Kashmir, Pakistan
[4]College of Engineering, Dhofar University, Salalah, Sultanate of Oman
[5]Faculty of Mechanical Engineering-Energy Division, K.N. Toosi University of Technology, Tehran, Iran.
[6]Department of Pharmaceutics and Pharmaceutical Technology Yarmouk University Irbid Jordan.
[7]School of Pharmaceutical Sciences Lovely Professional University Phagwara Punjab India.
[8]Biomaterials and Bioengineering Lab Translational Research Centre San Alberto Magno, Catholic University of Valencia San Vicente Mártir Valencia Spain.
[9]Department of Mechanical and Construction Engineering Northumbria University Newcastle upon Tyne UK.
[10]Department of Pharmaceutical Sciences Rangel College of Pharmacy, Texas A&M University Kingsville Texas USA.
[11]School of Pharmaceutical Sciences, Shoolini University of Biotechnology & Management Sciences, Solan, 173 212, India.
[12]Pharmacological and Diagnostic Research Centre, Al-Ahliyya Amman University, Faculty of Pharmacy, Amman, Jordan
[13]School of Pharmacy and Pharmaceutical Science Ulster University, Coleraine, Northern Ireland, UK.

Corresponding authors at:
Dr. Murtaza Tambuwala
m.tambuwala@ulster.ac.uk

Dr. Gowhar A. Naikoo
gahmed@du.edu.om

Dr. Israr U. Hassan
Dhofar University, Salalah, Sultanate of Oman
I_hassan@du.edu.om

Journal Pre-proof

Abstract

Nanotechnology is an arena of exploration and innovation concerned with building things generally, advancing resources and devices based on highly specific and superior nanomaterials with unmatched properties dependent on their morphology and diameter. 2D materials such as graphene have unique properties and applications varying from imaging, delivery of drugs, and theranostics of diseases. Each 2D material, ranging from the graphene family, MXenes, chalcogenides, and 2D oxides, have a unique potential based on their shape and morphology. In addition, 2D materials have intriguing physiochemical characteristics, increased aspect ratio and associated increased reactivity that make them an ideal contender in multiple applications. This review aims to answer the existing knowledge gaps in various 2D materials having interdisciplinary roles. We have presented a brief overview of the 2D materials, followed by their synthesis methods and techniques. We have also highlighted the different characterization methods used to characterize various 2D materials. Next, we performed an in-depth analysis of the potential toxicities of 2D materials to assess their risks in multiple applications. Lastly, we conclude our review by presenting the challenges and future perspectives of 2D materials as promising forerunners of science and technology.

Keywords: 2D materials; graphene; synthesis; characterization; toxicity

Journal Pre-proof

1. Introduction

The developing and promising field of nanotechnology signifies a multidisciplinary approach towards creating materials that can be measurable under 100 nm [1]. Nanomaterials (NMs) are entities with diameters between 1–1000 nm in any single dimension on a fundamental level. Nanowires, nanofibers, nanoplates, quantum dots are many nanoscale structures. The European Union Commission describes them as detached materials yet holds aggregated or agglomerated particles with external dimensions ranging between 1–100 nm [2]. Nanotechnology is a rapidly evolving field. Over the years, several NMs with different modifications like their shape, crystalline nature, size have been discovered, each displaying a unique property [3]. Because of their unique properties, NMs are applied in numerous fields, from medicinal to industrial. The utilization of nanomaterials is ever-expanding for commercial purposes, for example, pacifiers, fillers, restorative fixings, water filtration agents, electronic parts, semiconductors, and others [4]. In addition, these materials are also used in biomedical applications like nanomedicines, bioelectronics, cosmetics, biochips, and biosensors [5].

2D materials are significant among the different nanomaterials and play diverse roles in several fields. These are crystalline materials with a few atomic layers and possess strong interatomic interactions that are stronger than stacking interactions. Over a thousand 2D material structures have been discovered and sorted into several single or multi-layered structures, each displaying a different physicochemical property [6]. 2D materials like graphene, MoS_2, hexagon boron nitride have received widespread attention in recent years [7–9], each possessing unique properties. For instance, graphene demonstrates unmatched strength [10], enhanced thermal conductivity [11] and carrier mobility [12], and superior optical activities [13]. Also, graphene possesses zero bandgaps and have metal-like properties. Because of these exceptional properties, graphene is used in many applications, including field-effect transistors [14], photodetectors [15,16], and energy storage materials [17,18], in sensing technology [19], during drug delivery [20], and others. On the contrary, 2D materials like phosphorene demonstrate high flexibility, can be exfoliated, are highly stable, and possess a high bandgap [21]. Likewise, other 2D materials contain varying band gaps. For example, materials like WSe_2 [22], MoS_2 [23], and boron nitride [24] have direct band gaps and can be used in applications like transistors, optical devices, and photodetectors. On the other hand, materials like VS_2 [25] and borophene [26] have promising potential in energy storage materials, while stanene demonstrates potential in superconductors [27]. **Fig. 1** discusses the overview of the 2D materials, including the several types of 2D layered materials that have been studied in recent years.

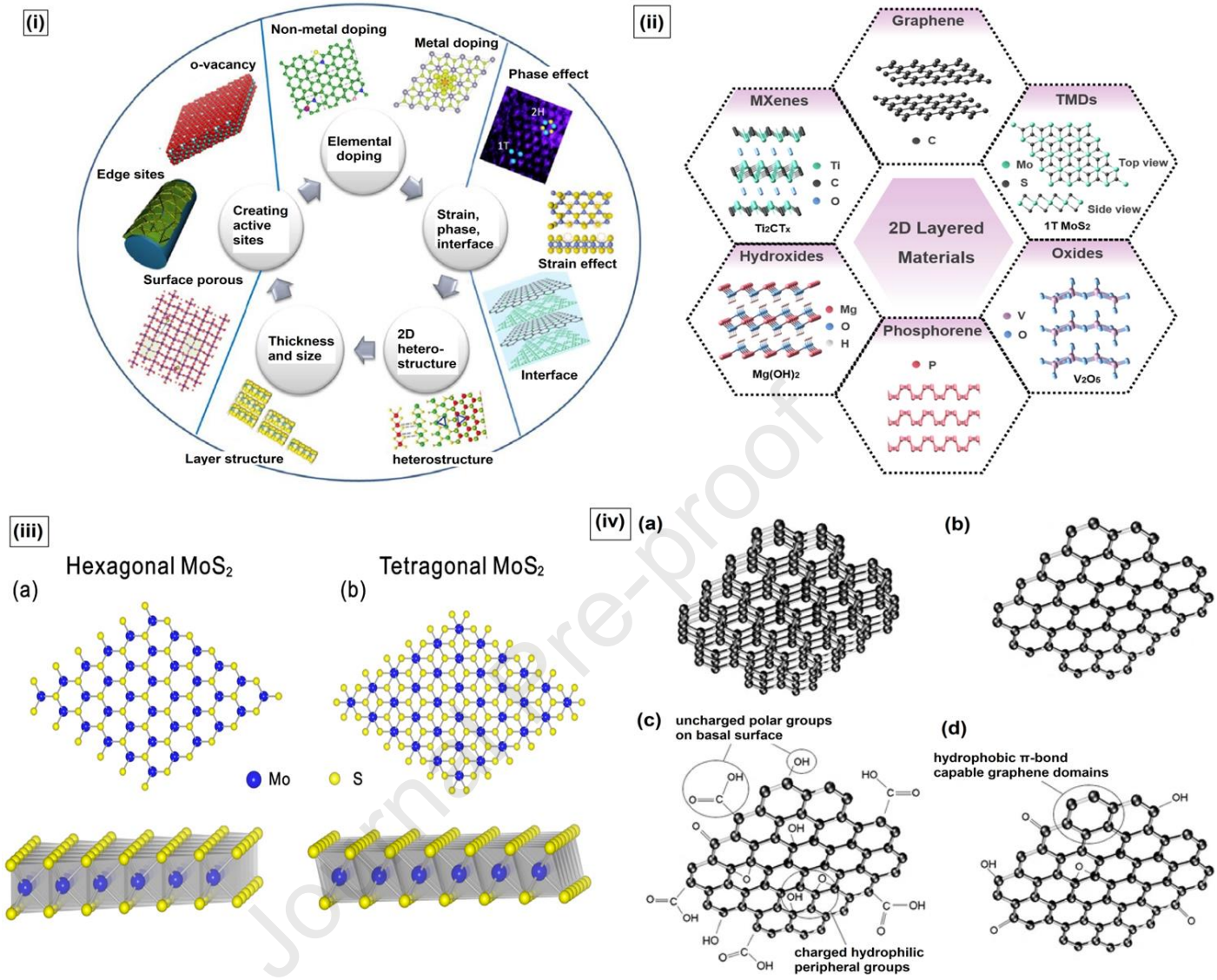

Fig. 1: Overview of 2-D nanomaterials. (i) Schematic illustration of 2D nanomaterials including carbon-based nanomaterials, silicate clays, LDHs, TMDs, TMOs, BP, g-C_3N_4, h-BN, AM, B NSs and SnTe NSs. Adapted with permission from ref. [28], copyright@2019 (Elsevier). **(ii)** Schematics of several typical types of two-dimensional-layered materials that have been widely studied recently. Adapted with permission from ref. [29], copyright@2019 (Wiley). **(iii)** Schematic diagram of the crystal structures of **(a)** monolayer hexagonal MoS_2 and **(b)** tetragonal MoS_2. Adapted with permission from ref. [30], copyright@2016 (Elsevier). **(iv)** Members of the graphene family materials: **(a)** few-layered graphene, **(b)** graphene nanosheet, **(c)** graphene oxide, and **(d)** reduced graphene. Adapted with permission from ref. [31], copyright@2012 (Nature).

Despite their vast potential and varying useful functions **(Fig. 2)**, the toxicological effects of 2D materials may drastically affect human well-being [32]. Though most of their toxicity is known, the exact size or concentration of 2D materials that play a crucial role in exhibiting these toxicological properties is unknown [33]. In recent years, though several literature review articles and research papers have been published, very few of them have discussed the toxicity of such materials. This information is necessary for the restricted development and usage of such NMs. Therefore, a comprehensive overview of accessible toxicity assessments of 2D materials has been presented in this article. This paper aims to understand the toxic potential of 2D materials like graphene family, Xenes, chalcogenides, and 2D oxides have been discussed in detail. In addition, we have also highlighted the synthesis and characterizations of NMs in the article.

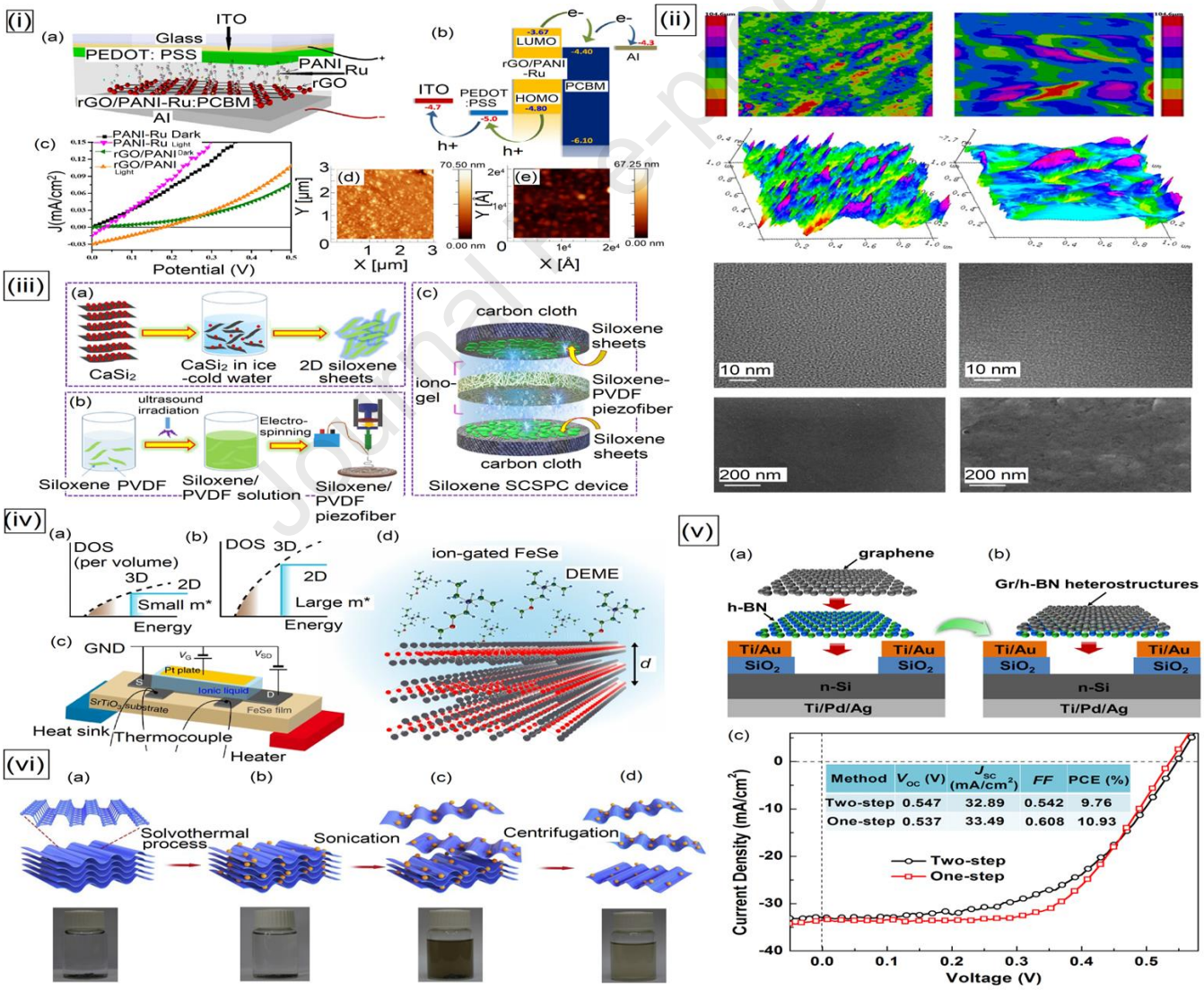

Method	V_{OC} (V)	J_{SC} (mA/cm^2)	*FF*	PCE (%)
Two-step	0.547	32.89	0.542	9.76
One-step	0.537	33.49	0.608	10.93

Fig. 2: Schematic overview of the functioning of 2-D- nanomaterials. (i) (a) Schematic diagram of PSC device fabricated using rGO/PANI-Ru as an electron donor, (b) Energy level diagram of rGO/PANI-Ru in PSC, (c) current density-voltage (J-V) characteristics of PSC device using PANI-Ru and rGO/PANI-Ru nanocomposites as an electron donor and (d and e) Tapping mode AFM image of PANI-Ru:PCBM and rGO/PANI-Ru:PCBM films. Adapted with permission from ref. [34], copyright@2017 (Nature) **(ii)** (a) AFM roughness image of GF. (b) AFM roughness image of GFPC 1. (c) AFM 3D image of GF. (d) AFM 3D image of GFPC 1. (e) HRTEM image of GF. (f) HRTEM image of GFPC 1. (g) SEM image of GF. (h) SEM image of GFPC 1. Adapted with permission from ref. [35], copyright@2018 (Nature). **(iii)** Schematic representation of steps involved in the fabrication of siloxene SCSPC. (a) represents the preparation of siloxene sheets via topochemical deintercalation of calcium from $CaSi_2$ in the presence of ice-cold HCl solution, (b) represents the fabrication process involved in the electrospinning of siloxene/PVDF piezofibers, and (c) indicates the fabrication of a siloxene SCSPC device using siloxene sheets-coated carbon cloth as two symmetric electrodes and electrospun siloxene–PVDF piezofibers impregnated with ionogel electrolyte as the separator. Adapted with permission from ref. [36], copyright@2020 (Nature). **(iv)** Schematic device structure for thermoelectric measurement. (a) Schematic illustration of the electronic density of states (DOS) for three-dimensional (3D) and two-dimensional (2D) electrons. (b) The large effective mass m^* enhances the DOS, which is favorable to the enhancement of the Seebeck effect. (c) Device structure for thermoelectric measurement. V_{SD} and V_G stand for the source (S)−drain (D) voltage and the gate bias voltage, respectively. When V_G is applied to the Pt plate, ions in the ionic liquid are redistributed, forming an electric double layer on the surface of the FeSe film. (d) Enlarged illustration of the ionic liquid/FeSe interface. Under the positive gate bias, *N*,*N*-diethyl-*N*-(2-methoxyethyl)-*N*-methylammonium cations, $DEME^+$, align on the surface of FeSe. The thickness *d* of the FeSe thin film was tuned by electrochemical etching. Adapted with permission from ref. [37], copyright@2019 (Nature). **(v)** Schematic illustrations of the Gr/h-BN/Si solar cells fabricated by (a) the two-step method and (b) the one-step method. (c) Illuminated J-V characteristics of Gr/h-BN/Si solar cells fabricated by using the one-step and two-step method. The inserted table summarizes the corresponding photovoltaic parameters of the solar cells. In both devices the graphene films were co-doped by Au NPs and HNO_3 vapor. Adapted with permission from ref. [38], copyright@2016 (Elsevier). **(vi)** Schematic illustration of solvothermal-assisted exfoliation and optical photo of dispersion of BP sheets in ACN: Bulk BP (a), insertion of ACN molecules into the interlayers of BP (b), exfoliated BP sheets dispersed in ACN (c), the obtained few-layer BP nanosheets (d). Adapted with permission from ref. [39], copyright@2018 (Elsevier).

2. Synthesis of 2D Materials:

The 2D materials are synthesized via different techniques, primarily using the bottom up or the top-down methods. The bottom-up is based on creating nanomaterial from other atoms or molecules. The following techniques are used in 2D material fabrication: sol-gel, chemical vapour deposition (CVD), and biosynthesis. The bottom-up synthesis crucially depends on the growth substrate. Thus, these substrates must be thoroughly studied for compatibility with the required 2D material [40]. The sol-gel method is a widely used bottom-up method for NMs development because of the relatively straightforward process. Large quantities of NMs can be fabricated from this process. Sol-gel is a chemical pathway that uses a chemical solution (sol) to produce an interlinked unit of discrete particles (gel). Chlorides and oxides of metals are the most preferred starting materials in this process[41]. The starting material is added into the host liquid using various techniques like stirring, shaking or sonication, resulting in the gel's formation. Several techniques like filtration, sedimentation and centrifugation recover the nanoparticles [42].

The other synthesis method is spinning. An instrument spinning disc reactor (SDR) is used to synthesize NMs by spinning. SDR hosts a spinning disc within a reactor such that the physical parameters can be monitored in this chamber. Nitrogen or any inert gas is added to a chamber to remove oxygen inside. Next, the precursor and water are added while the disc moves at varying speeds. The rotation results in a combination of core atoms, and they are separated, taken out and dried [43]. The third synthesis method is the chemical vapour deposition that produces tough, highly pure and robust NMs. In this method, the NMs are synthesized by settling a thin layer of gaseous reactants on the substrate. This reaction occurs at room temperature. This chemical reaction results in the deposition of a thin layer of the final product on the substrate's surface, which is then collected. The most frequently employed method for large production of NMs is pyrolysis. It includes burning a starter – either liquid or vapour with flame. The precursor is subjected to the furnace at high pressure through a small opening where it combusts [44,45]. The nanoparticles are recovered from by-product gases in various ways. The benefits of pyrolysis are an efficient, simple, continuous process and cost-effective. On the other hand, biosynthesis is an eco-friendly method to produce nanoparticles that are biodegradable as well as non-toxic [46]. It utilizes microscopic organisms, fungi, plant-derived products, among others. The nanoparticles thus made have significant roles in biomedical applications **(Fig. 3)**.

Journal Pre-proof

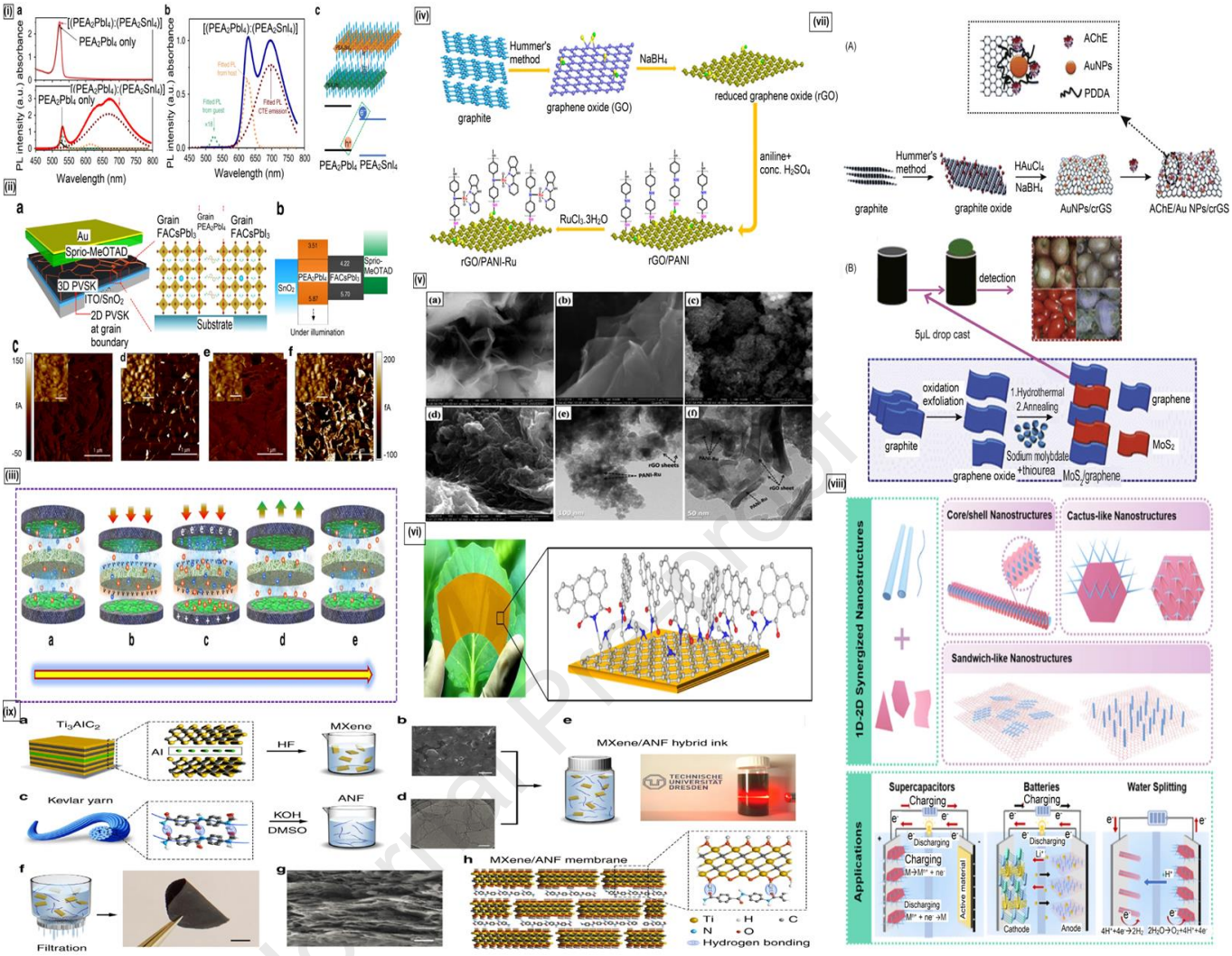

Fig. 3: Schematic overview of various 2-D nanomaterials, their applications, and characterizations. (i) Optical characteristics of CTE formation in 2D perovskite heterostructures. **(a)** Absorption and PL spectra are shown for 2D perovskite heterostructured [$(PEA_2PbI_4)0.999$:$(PEA_2SnI_4)0.001$] film. The absorption spectrum indicates that the bandgap is governed by the host (PEA_2PbI_4) component in the heterostructures. **(b)** PL spectrum is shown for 2D perovskite heterostructured [$(PEA_2SnI_4)0.999$:$(PEA_2PbI_4)0.001$] film after switching host and guest components. **(c)** Schematic diagram illustrates the formation of CTEs at the interfaces between PEA_2PbI_4 and PEA_2SnI_4 components in 2D perovskite heterostructures [$(PEA_2PbI_4)1-x$:$(PEA_2SnI_4)x$]. Adapted with permission from ref. [47], copyright@2020 (Nature). **(ii)** Band alignment and local conductivity with 2D perovskite. **(a)** Schematics of the device incorporating polycrystalline 3D perovskite film with 2D perovskite at grain boundaries and **(b)** band structure of each layer in device analyzed by ultraviolet photoelectron spectroscopy (UPS) and Tauc plots. Conductive atomic force microscopic (c-AFM) images of **(c, e)** bare $FAPbI_3$ and **(b, d)**

with 2D perovskite films on SnO**2** coated ITO glass. The measurement was carried out with bias voltage of 100 mV under **(c, d)** room light or **(d, f)** low intensity light illumination provided by the AFM setup. Inset of each image shows corresponding topology of the films. Scale bar at left side is for **(c)** and **(d)** while at right side is for **(e)** and **(f)**. Adapted with permission from ref. [48], copyright@2018 (Nature). **(iii)** Schematic illustration of the working mechanism of the siloxene SCSPC device. **(a)** The initial state of the siloxene SCSPC device with no applied compressive force. **(b)** With an applied compressive force to the siloxene SCSPC device, the siloxene/PVDF creates a piezoelectric potential that drives the electrolyte ions towards the electrode surface. **(c)** An equilibrium state has been reached between the piezoelectric potential created and the electrochemical reaction of the siloxene SCSPC device. **(d)** State of siloxene SCSPC when the compressive force is stopped, i.e., the disappearance of piezoelectric potential and leads to attaining the equilibrium state. **(e)** State of siloxene SCSPC after completion of one self-charging cycle. Adapted with permission from ref. [36], copyright@2020 (Nature). **(iv)** Synthesis procedure of rGO/PANI-Ru hybrid nanocomposite. **(v)** FE-SEM image of **(a)** GO, **(b)** rGO, **(c)** PANI-Ru, **(d)** rGO/PANI-Ru and **(e and f)** TEM image of rGO/PANI-Ru nanocomposite with different magnification. Adapted with permission from ref. [34], copyright@2017 (Nature). **(vi)** Photograph of GFPC 1 along with the detailed structure (gray = C; red = O; blue = N). Adapted with permission from ref. [35], copyright@2018 (Nature). **(vii) (A)** Schematic illustration of AChE/AuNPs/cr-Gs nanoassembly generation by using PDDA for pesticide detection. **(B)** A reliable and robust methyl parathion sensor has been developed using heterostructured MoS_2/graphene. Adapted with permission from ref. [49], copyright@2018 (Elsevier). **(viii)** Schematic of three categories of 1D-2D synergized nanostructures. Adapted with permission from ref. [29], copyright@2019 (Wiley). **(ix)** Schematic representation of steps involved in the fabrication of siloxene SCSPC. **(a)** represents the preparation of siloxene sheets via topochemical deintercalation of calcium from $CaSi_2$ in the presence of ice-cold HCl solution, **(b)** represents the fabrication process involved in the electrospinning of siloxene/PVDF piezofibers, and **(c)** indicates the fabrication of a siloxene SCSPC device using siloxene sheets-coated carbon cloth as two symmetric electrodes and electrospun siloxene–PVDF piezofibers impregnated with ionogel electrolyte as the separator. Adapted with permission from ref. [36], copyright@2020 (Nature).

2D materials are synthesized via the top-down method, which involves the breakdown of a larger entity into nano-sized substances. Nanolithography, mechanical milling, laser ablation, thermal decomposition, and sputtering are the most extensively applied top-down procedures for synthesizing NMs. Mechanical milling is utilized for grinding and post-annealing nanomaterials [50]: plastic deformation, fracture, and cold-welding influence mechanical milling to develop different kinds of nanoparticles. Lithography is used to create nanoparticles with a particular pattern or structure imprinted on them. This property makes

this method a highly reliable way to develop nanoparticles. This method's drawbacks are the requirement of complex types of machinery and high expenses [51]. Laser ablation is another synthesis method, which involves a beam that condenses a plasma plane after treatment with metal in a liquid solution [52]. The main advantage of LASIS is the production of NMs within the water and organic solvents, which do not require chemicals. Due to this characteristic, it is an environmentally friendly process. In yet another technique, sputtering, minute concentrations of NPs are layered on an intermediate accompanied with annealing. Some of the elements affecting the 2D materials' diameter and shape are the temperature range, surface type, and time taken for annealing [53]. Another top-down method includes thermal decomposition, which breaks the chemical bonds in the compound by heat [54]. The NMs are created by breaking metal at particular temperatures. The secondary products are made from NMs by undergoing a chemical reaction.

Though 2D materials can be synthesised via either of the techniques mentioned above, in general, 2D materials are obtained by either of the following methods: physical vapour deposition (PVD), scotch tape method (micromechanical cleavage), or by CVD. During micromechanical division, massive crystalline structures are broken down into single or multi-layered samples and are used in micro-sized electrical and optical apparatus. The size and shape of the sheets exfoliated can be carefully monitored and controlled using various exfoliation methods [55]. The major drawback of this technique is that it is time-consuming and requires skilled professionals to do the work. In addition, this method is ideal for developing layered 2D materials. For instance, this method can exfoliate bulk allotrope like graphite to graphene. Thus, this method is limited to producing limited 2D materials only [56,57]. However, this method can become more inclusive via exfoliation procedures that use solutions instead of crystalline structures [58] and this way, 2D material is produced in hefty amounts.

On the other hand, the PVD method uses a heat source that monitors the deposition of materials on the substrates [59]. To develop synthetic elemental 2D materials, PVD uses an ultrahigh vacuum environment and a highly pure atomic source. In the CVD process, the chemical reaction of gaseous, liquid, and solid materials under a highly regulated environment produces 2D materials [60,61]. The mechanism of action during this process differs with each substrate; substrates that possess low insolubility perform the catalysis of self-limiting development of very thin sheets of atomic size. On the contrary, substrates with high precursor solubility dissolve large quantities of the substrates that separate when cooled. This segregation makes the use of solid-state precursors by the growing substrate. The development of 2D materials happens when the substrate is warmed up to switch on the sublimation or the diffusion action and thus develops a sheet on the surface that is rich in the precursor. After this, it undergoes condensation to form the 2D phase material. However, the substrate chosen depends on the ones that possess a

precursor element like during the development of epitaxial graphene on SiC [62]. Therefore, for the synthesis and growth of any 2D materials, the reactions with the substrates are essential [40,63]. **Fig. 4** shows the various synthesis methods for different 2D materials, including the development of graphene and hBN via CVD and synthetic steps of GA-MNPs and LMNPs via non-ionic reverse micelle methods.

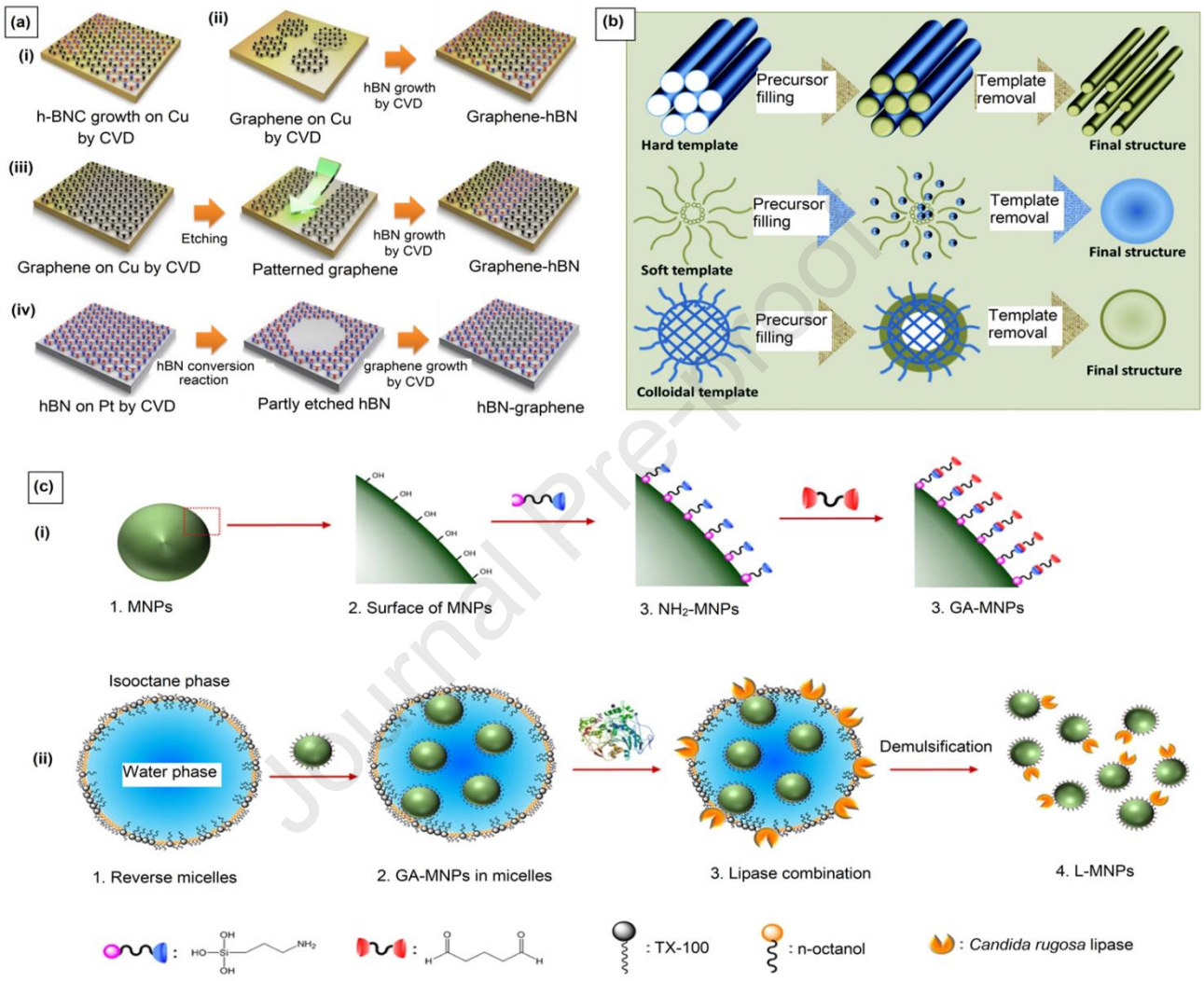

Fig. 4: Synthesis of various 2-D- nanomaterials (a) Schematic growth of in-plane graphene and hBN heterostructures by various techniques. **(i)** Simultaneous in situ CVD growth, **(ii)** Sequential in situ CVD growth. **(iii)** Lithography-assisted growth and **(iv)** Conversion growth. Adapted with permission from ref [64], copyright@2016 (Elsevier) **(b)** Schematic representation of the synthesis of materials using different types of templates. Adapted with permission from ref. [65], copyright@2020 (Royal Society Chemistry) **(c) (i)** Schematic showing the synthetic steps of the GA-MNPs. **(ii)** Synthesis of L-MNPs through the non-ionic reverse micelle method. Adapted with permission from ref. [66], copyright@2017 (Nature).

3. Characterization of 2D Materials:

Various techniques have been used to characterise 2D materials, and each provides information about morphological, structural, particle size, surface area, and optical properties of the material. Microscopic techniques, namely TEM, SEM, and polarized optical microscopy (POM), are most widely used. The fundamental properties of 2D materials are analyzed using standard techniques such as XRD, energy dispersive X-ray (EDX), XPS, Raman, BET, and Zeta size analyzer, among other methods. The essential technique in analyzing the systemic and conformational characteristics of 2D materials is XRD. It provides enough information about the phase (single and multiple) and crystallinity of NMs. Methods like XRD, AFM, SEM and TEM can indicate the diameter of 2D materials. UV-Vis, DRS, and photoluminescence (PL) techniques help understand optical properties like the absorption, reflection, and phosphorescence of 2D materials [67,68].

3.1. Characterization of graphene family

Characterization of graphene, like any other characterization procedure is essential to study the properties of graphene, morphology, limitations, and the number of layers in the molecule using varying techniques, like microscopic and spectroscopic assays [69,70]. The most commonly used techniques for the characterization of the graphene family include Raman spectroscopy, SEM, TEM, XRD, and UV-vis spectroscopy.

Monochromatic laser-based Raman spectroscopy is used to analyze and study the quality and layers of graphene and its derivatives structure. During this, atomic or often molecular vibrations are produced, which causes changes in the laser energy of the molecules. This, in turn, leads to the formation of different peaks depending on the molecule [71,72]. The peak intensity ratio gives an idea of the number of layers or any disorders in graphene molecules [73,74]. With an increasing proportion, the number of graphene layers decreases. On the contrary, UV-Vis spectroscopy is used to study the kind of graphene molecule (graphene oxide, reduced graphene oxide or pristine graphene) and the number of layers in the molecule. The absorbance results are obtained due to the electron transfer at the carbon pi bonds (pi to pi* transitions) [75]. The number of layers or the width of the molecule is analyzed via ultraviolet transmittance. When the number of layers in the graphene molecule increases, the transmittance reduces [76]. The other technique used to characterise the graphene family is the TEM utilised to examine the quality of the graphene and the number of layers within the molecules. The results are obtained by the transmittance of the electron beam through the molecule to be studied. SEM is also widely used to analyse any impurities, unevenness or folding within graphene molecules. On the other hand, XRD studies unit cell dimensions of the molecule and thus performs the phase identification of the substance.

The examples of different characterization methods, including XRD pattern, SAED pattern, lattice fringes, SEM and TEM images for various 2D materials, have been shown in **Fig. 5**.

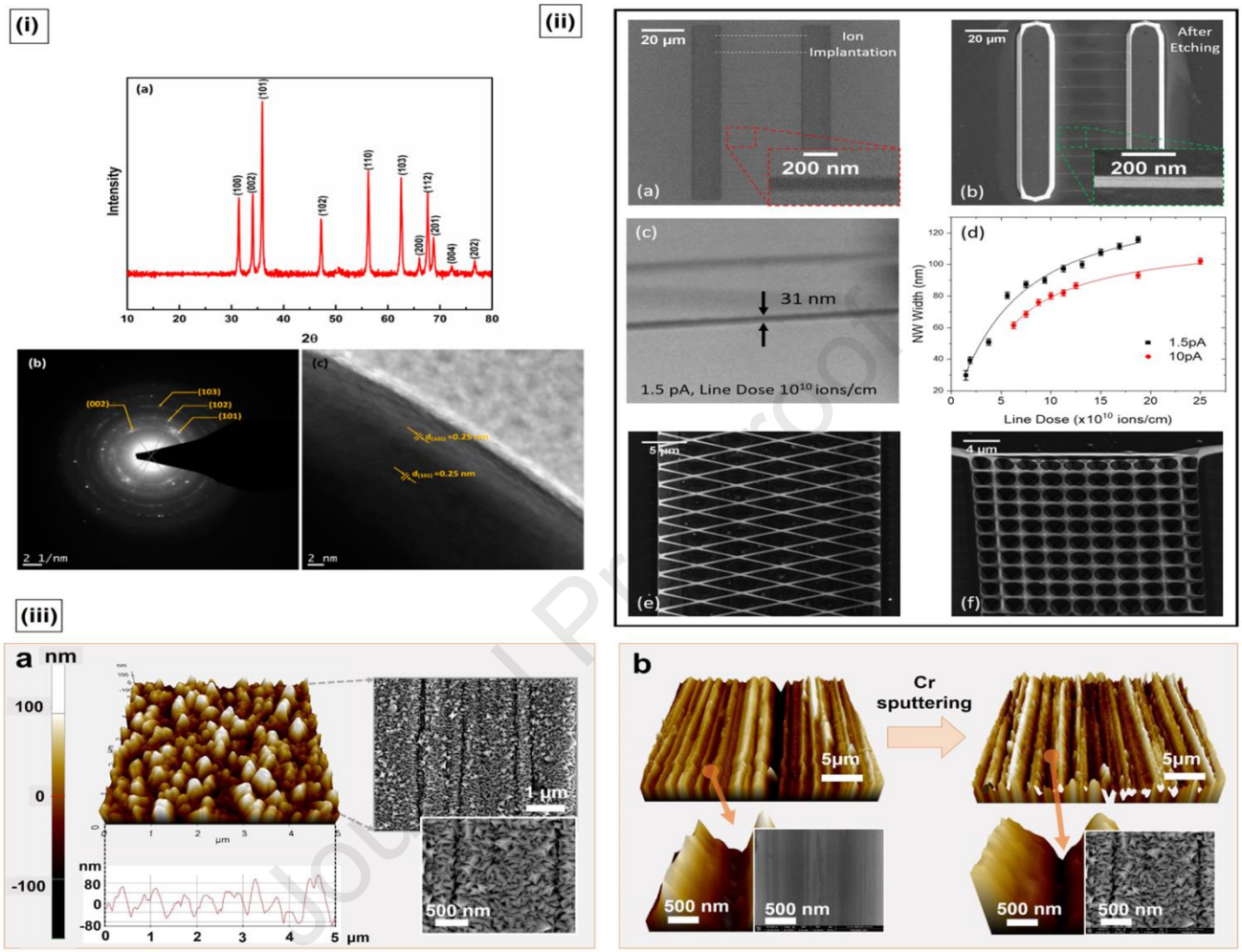

Fig. 5: Characterization of 2-D nanomaterials. (i) (a) XRD pattern (b) SAED pattern and (c) lattice fringes of as-synthesized ZnO nanoparticles. Adapted with permission from ref. [77], copyright@2018 (MDPI). **(ii)** Fabrication of suspended Si nanowires: (a) SEM image of implanted Si for fabrication of nanowires (b) fabricated high aspect ratio (~625) suspended Si nanowires with length ~25 μm; inset in (a) and (b) show SEM magnified representative SEM image of implanted line profile and fabricated NW, (c) A high resolution SEM image of a Si NW, demonstrating the NW down to ~31 nm, (d) Evolution of NW width against implantation line dose at 1.5, 10 pA beam current; SEM images of fabricated suspended Si: (e) Rectangular, (f) Circular mesh. Adapted with permission from ref. [78], copyright@2020 (Elsevier). **(iii)** TEM images of (a) GA-MNPs and (b) L-MNPs. (c) Change of surface morphologies before and after DC sputtering: (a) Nanoscale roughness of Cr-SP4000 (5×5 μm^2 in AFM resolution).

(b) Microscale roughness and capillary flow channels (30 × 30 μm^2 in AFM resolution). Adapted with permission from ref [79], copyright@2017 (Elsevier).

3.2. Characterization of MXenes

2D transition metal carbonitrides, usually referred to as MXenes, are often characterized visually. When the precursor transforms itself into MXene molecule, there is an observation of colour change that is very distinctive. The precursors are usually grey coloured, and the products given possess different colours that are dependent on the overall structure and composition of the molecules [80]. The most commonly used characterization techniques employed for the characterization of MXenes include XRD and SEM. Among the two, XRD quickly confirms the MXene production [80]. When the precursor is converted into multiple layered MXene, characteristic XRD patterns are obtained for that 2D material. Also, due to the hydrophilic nature of MXenes, the spaces between the layers within the structures are wide enough to include intercalating agents, which influences the XRD patterns produced [81]. In addition, XRD gives an idea on the electrochemistry of the reaction taking place on the MXene surface during any electrochemical reactions. Thus, XRD improves our ability to understand MXenes and how their properties can be exploited in different fields.

The SEM technique aids in the visualization of MXene structure formation, gives a detailed overview of the structure of the 2D material produced. Often EDS is used along with SEM to provide better qualitative and quantitative data about the molecule [80]. Other techniques like pair distribution function (PDF) analysis [82], X-ray absorption spectroscopy (XAS), and atomic force microscopy (AFM) methods are also used to analyze MXenes. The PDF studies give information about the surface groups attached to the MXenes [83], the influence of etching on these 2D materials [84], and the precise location of the different atoms within the MXene molecule [85]. The other method used for MXene characterization of the XAS uses synchrotron radiation that acts as a bright X-ray source and helps study the electronic structure of these 2D materials at the primary level [80]. This technique helps analyze the adsorption and other catalytic reactions that occur at the surface of MXenes [86].

3.3. Characterization of chalcogenides

Characterization of chalcogenides is generally done using optical, structural, compositional, and electrical methods, including XRD, EDS, FESEM, UV-Vis, differential scanning calorimetric method, and dielectric spectroscopy. XRD helps identify the crystal phase and gives an in-depth analysis of the dimensions of the 2D material [87]. With this technique, the structural analysis of complete crystals or even thin sheets of 2D materials is done to study the overall morphology of the material, its geometry and

orientation and the lattice constraints within the molecule. The XRD pattern produced is then compared with the existing data on the given structure, enabling us to understand the chalcogenides better [88]. EDAX is also an instrumental technique to characterise chalcogenides and is often used along with FESEM to study the elemental or chemical composition of chalcogenides [89]. It gives the quantitative analysis of large crystals and thin sheets of 2D material. The other technique used is FESEM, which uses a field emission gun that produces better resolution images even under small accelerating voltages, giving better results than typical SEM imaging [90].

Among the optical characterization techniques is UV-Vis spectroscopy, which quantifies the light absorbed and deflected by the material. This method is advantageous to study the stability of the chalcogenides [91]. At the same time, photoluminescence spectroscopy gives an idea about the overall electronic structure of the chalcogenides, any persistent impurities or disorders within the structure [92]. Furthermore, the differential scanning calorimetric method gives details like the kinetic parameters of the 2D material and allows for the study of fusion and crystallization events of chalcogenides [93]. On the other hand, dielectric spectroscopy measures the dielectric properties of the chalcogenides and gives an idea of the molecular structure of the material. In addition, this method also helps understand the molecular mechanisms, dielectric properties, and any impurity within the structure [94].

3.4. Characterization of 2D oxides

The most commonly used characterization techniques to study 2D oxides include the AFM, Raman spectroscopy, and TEM. The methods AFM and TEM help analyze the structure and stability of the 2D oxides [95]. In addition, Raman spectroscopy is also used to study the vibrational spectra and the phonon modes and the crystalline axes of the 2D oxides [96]. These characterization techniques help check both bulky crystals and thin sheets of the 2D-oxides, thereby giving precise quantitative and qualitative characterization results of the various 2D oxides. The examples of different characterization techniques including TEM, FESEM, and AFM imaging of various 2D materials can be seen in **Fig. 6**.

Journal Pre-proof

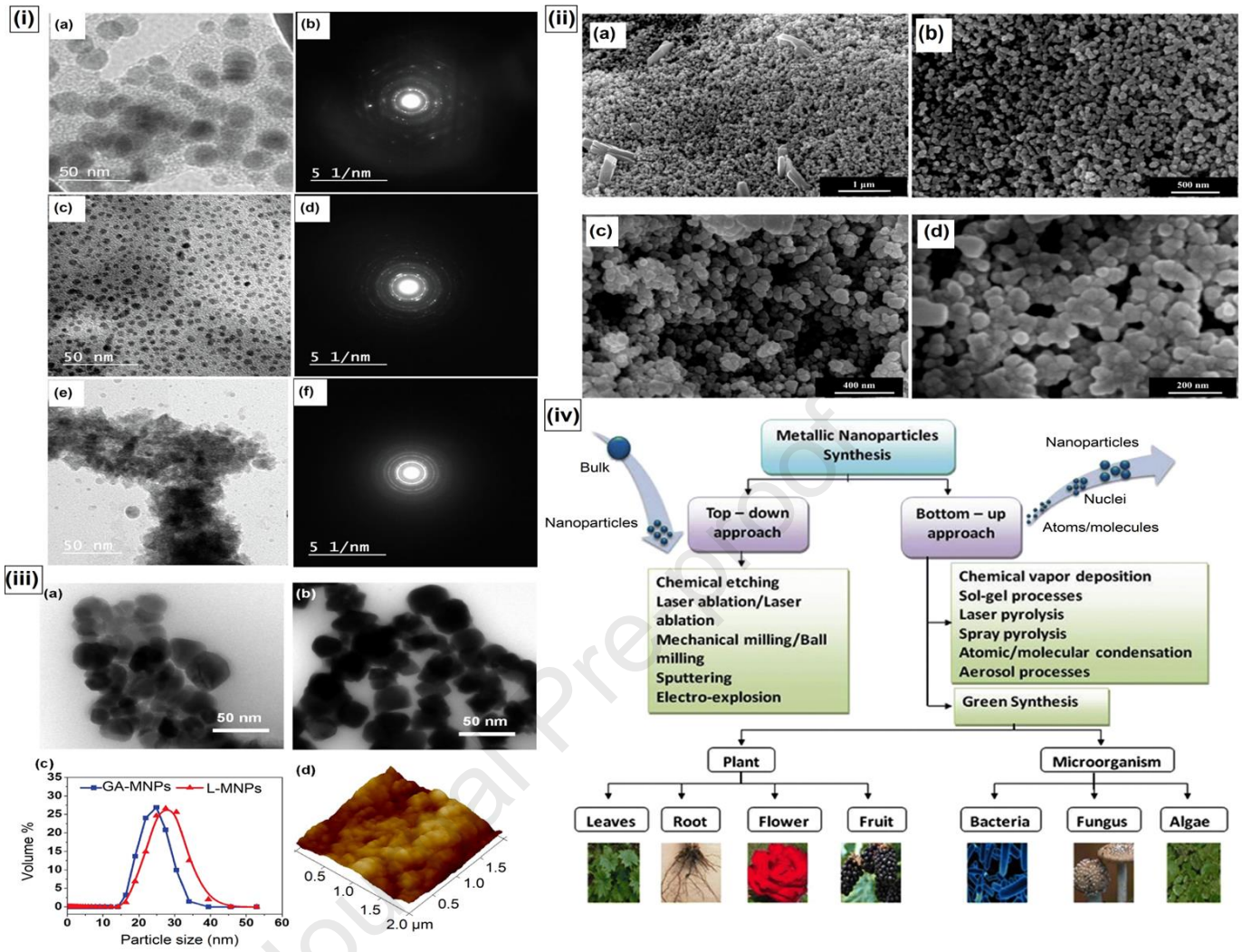

Fig. 6: Characterization techniques of various 2-D- nanomaterials. (i) TEM images of copper nanoparticles prepared by gradual addition of L-ascorbic acid (3 ml/min) from different 0.5 M ammoniacal leachant solutions:(A, B) amm. citrate; (C, D) amm. carbonate; (E, F) amm. chloride at the optimum leaching conditions. Adapted with permission from ref. [97], copyright@2020 (Elsevier). **(ii)** FESEM images of ZnO nanoparticles at different magnification (a) 65,000×; (b) 120,000×; (c) 200,000×; and (d) 350,000×. Adapted with permission from ref. [77], copyright@2018 (MDPI). **(iii)** Particle size distribution curves of GA-MNPs and L-MNPs. (d) AFM topographic image of the L-MNPs in an small area of 2×2 μm^2. Adapted with permission from ref. [66], copyright@2017 (Nature). **(iv)** Different synthesis approaches available for the preparation of metal nanoparticles. Adapted with permission from ref. [98], copyright@2018 (Springer Nature).

4. Toxicity of 2D materials

The majority of the recent studies on 2D materials have been primarily on their synthesis methods, stability **(Fig. 7)** and the various characterization techniques to study their electrochemical properties and unique behavioural aspects [99]. However, understanding the biochemical and ecological Furthermore, risk characterization of 2D materials is essential so that potential uncertainties and any hindrances to their development, commercialization, and applications can be avoided.

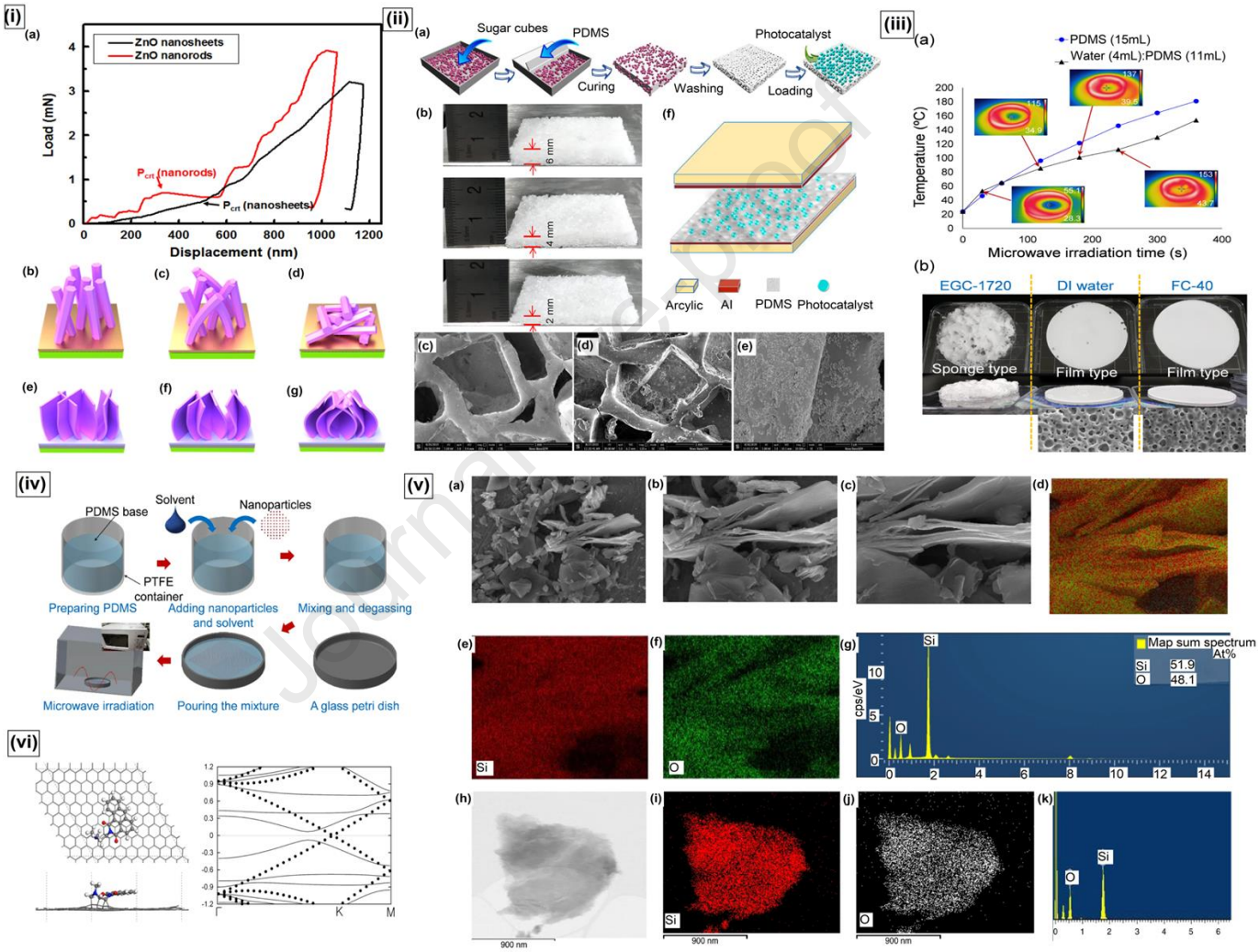

Fig. 7: Stability of various 2-D nanomaterials. (i) Mechanical stability of ZnO nanorods and nanosheets. (a) Load-displacement curve of ZnO nanosheets and nanorods using nanoindentor. Nanoindentation testing gives insight into the ZnO nanorods and nanosheets which respond differently under uniaxial compression. (b–d) and (e–g), Schematic images describing the morphological development of ZnO nanorods and nanosheets, respectively, according to the applying load of below and

above P_{crt}. Adapted with permission from ref. [100], copyright@2013 (Nature). **(ii)** (a) A schematic shows the preparation process of the TiO_2/PDMS sponge layer. (b) Digital photographs of different thickness of the spongy PDMS layer loaded with photocatalyst TiO_2 NPs. SEM images of the microstructure of (c) PDMS and (d–e) TiO_2/PDMS sponge. (f) Schematic of the CS-TENG with photocatalyst-loaded PDMS spongy as friction layer. Adapted with permission from ref. [101], copyright@2020 (Elsevier). **(iii)** (a) Temperature variation of PDMS precursor during MW irradiation. (b) Photograph and FE-SEM images of fabricated porous PDMS. **(iv)** A schematic diagram of fabrication process. Adapted with permission from ref. [102], copyright@2018 (Nature). **(v)** Morphological and elemental analysis of siloxene sheets. (a–c) Field emission scanning electron micrographs of the siloxene sheets. (d) Elemental mapping analysis showing the overlay map and (e–f) EDS mapping of Si and O present in the siloxene sheets; (g) EDS spectrum of Si and O present in siloxene sheets; (h) high-resolution transmission electron micrograph of individual siloxene sheets; (i, j) EDS mapping of Si, and O elements present in the siloxene sheets; and (k) elemental composition spectrum of Si and O present in siloxene sheets. Adapted with permission from ref. [36], copyright@2020 (Nature). **(vi)** The optimized atomic geometry and the electronic band structure of GFPC 1. (a) Top-view and (b) side-view of GFPC 1. Note the π-π stacking between aromatic rings in DdIC chromophore and graphene. (c) The electronic band structure of GFPC 1 photocatalytic system. The electronic band of pristine graphene is also shown with circles. The hybridization between molecular orbitals in chromophore and graphene is noticeable around K point. The Dirac point of graphene lies around the center of HOMO-LUMO gap of the chromophore. Adapted with permission from ref. [35], copyright@2018 (Nature).

4.1. Toxicity of graphene family

The potential toxic properties of 2D materials constitute a significant concern for scientists and the research field. Because of their small size, these materials can easily be transported and accumulated in cells and related structures over time. In the past decade, graphene has gained much attention from the scientific community. Therefore, the toxic behaviour of graphene in biological systems is a fundamental issue that needs particular focus. Currently, several different groups have researched the effects of graphene-based materials on bacterial growth. Unfortunately, observed results may be inconsistent due to other experimental conditions and material preparations. Many studies have also shown the biodistribution and *in vivo* toxicology of graphene and its derivatives functionalized through different animal administration routes. For instance, Liu and colleagues have conducted a dose and size-dependent toxicity and biodistribution of GO [103]. They noted that S-GO was primarily deposited in the liver, and there were few aggregates in the lung and spleen. Compared with s-GO, I-GO showed more accumulation in the lungs and had a residual amount of about 19% after 180 minutes. TEM analysis of the lungs

showed that s-GO in phagocytes accumulated in the cells, while 1-GO particles (greater than 1 µm) were placed in the lung cell space.

In yet another study, Strojny and colleagues studied the intraperitoneal toxicity of GO, graphite and nanodiamonds in 6-week-old female Wistar rats [104]. The NP suspension was introduced at a 4 mg/kg dose at three days for 4 or 12 weeks. After 1-3 months, the mice were euthanized, and the liver and blood were taken for further studies. The authors observed nanoparticle clusters in the peritoneal cavity near the site where it was injected. Smaller aggregates were seen in the mesenteric and liver serosal membranes, indicating that nanoparticles were transported and accumulated in the liver. At any time (4 weeks or 12 weeks), no further worsening of health was noted for either of the nanoparticles (GO, graphite or nanodiamond). Blood tests and liver enzyme levels are standard, indicating that the liver has good biocompatibility. Under the microscope, granulomatous reactions appear in the lungs, interstitial fibrosis, peri-scalp emphysema, necrosis, and severe vascular sclerosis appear [105]. Rarely, extensive tissue necrosis results in large cavities filled with black fatty fluid. Non-asbestos objects with black graphite cores are similar to the characteristic iron-containing things observed after asbestos exposure, distributed in the lungs and sometimes found in sputum [106].

In a closely similar study, Hu and group studied the antibacterial activity of GO and rGO on *E. coli* cells at concentrations of 0, 20, and 85 µg/ml [107]. It was found that the metabolic activity of *E. coli* was reduced to ~70% and ~13%, respectively. RGO has an incubation time of 2 hours and shows antibacterial activity. The coliform bacteria containing 85 µg/ml rGO solutions can only produce 24% of cell viability. MET studies have shown that cell integrity is lost after exposure to GO and rGO due to physical damage to the cell membrane. Also, cells grown on GO and rGO paper can damage bacterial cell membranes. The authors concluded that the charge transfer between the graphene's basal plane and the bacterial cell body caused the antibacterial effect. When evaluating the effect of common wheat on growth, similar results were obtained that reported the graphene's adverse effects. In addition to inhibiting growth, graphene also disrupts photosynthesis. Furthermore, it leads to an imbalance of nutritional homeostasis, which is manifested by reduced shoot biomass and root hair numbers, reduced chlorophyll content and PSII activity, and nutrient deficiency [108]. From the above results, it can be understood that graphene's physical and chemical properties, like the surface functional groups, fillers, coatings, size and structural defects, can affect its behaviour *in vitro*/*in vivo* and its toxicity to biological systems.

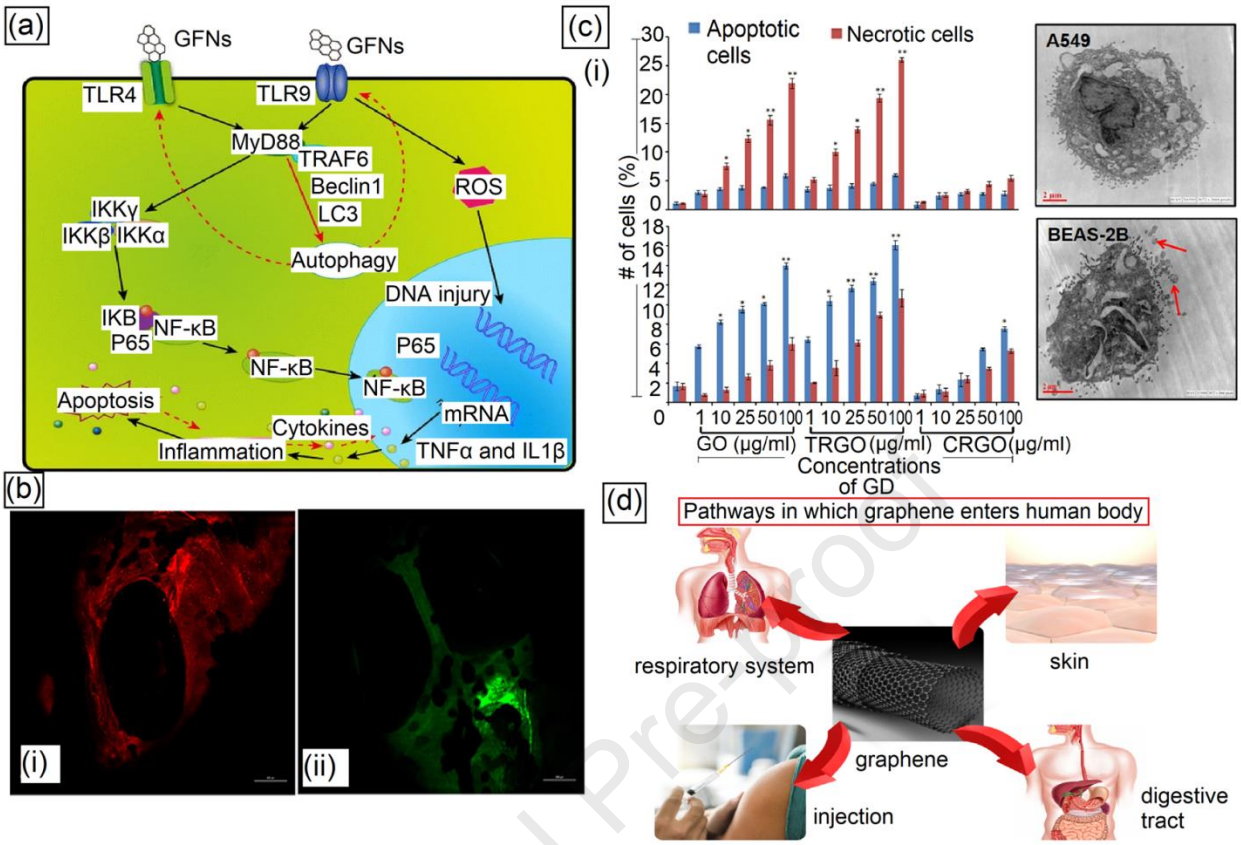

Fig. 8: Toxicity of graphene and its derivatives. (a) A schematic diagram elucidating signalling pathway of TLR4 and TLR9 responsible for GFNs-induced cytotoxicity. GFNs can be recognized by TLRs, thus activate IKK and IκB by a MyD88-dependent mechanism, resulting in the release of NF-κB subunits and initiating the translocation into the nucleus. Thus, pro-inflammatory factors were transcribed and secreted out of nucleus, modulating the immune responses initiating programmed autophagy, apoptosis and necrosis. Adapted with permission from ref. [109], copyright@2016 (Springer Nature). **(b)** Larvae zebrafish 96 hpf free GO treated. Zebrafish exposed to free GO showed a positive response to anti-HO-1 (i) and anti-iNOS (ii) in whole body. Adapted with permission from ref. [110], copyright@2018 (Frontiers**). (c)** Mode of cell death analysis in graphene derivatives exposed human lung cells. (i) Flow cytometry based Annexin V/PI assay showed a significant increase in necrotic cells in A549 (upper panel) whereas apoptotic cells increase in BEAS-2B (lower panel) after 24 h exposure. (ii) Representative TEM photomicrographs showing necrosis in A549 and apoptosis in BEAS-2B cells (red arrow – apoptotic bodies). Adapted with permission from ref. [111], copyright@2016 (Nature). **(d)** Pathways through graphene derivatives enter the human body.

4.2. Toxicity of MXenes

2D materials have several types of compounds and thus display different chemistries; this necessarily means that though a few of the chemistries involving these compounds may be safe and some may not [112]. The MXene are a volatile group of compounds and contain over thirty such compositions that have been explored so far [113]. However, only limited groups, including $Ti_3C_2T_x$ [114–117], $Nb_4C_3T_x$ [114], $Mo_2Ti_2C_3T_x$ [114], and a few others, have been studied in terms of their toxic potential and effects on the environment. So far, none of the studies has confirmed any adverse consequences or poisonous potential of MXenes on human or animal cells.

For instance, in a study by Jastrzębska and colleagues, it was seen that $Ti_3C_2T_x$ does not cause any cytotoxic effects up to concentrations of 500 μg mL^{-1} [118]. In a closely similar study by Han and colleagues, it was observed that prolonged exposure to high concentrations of $Ti_3C_2T_x$ (600 μg mL^{-1}) does not result in any cytotoxic conditions [119]. Another study by Nasrallah *et al.* on zebra-fishes confirmed that this MXene is 'practically non-toxic' [120]. Feng *et al.*, in their research on Mo_2CT_x, also observed no cytotoxic effects on normal cells or cancer cells even on prolonged exposure, even when the MXene was taken in large concentrations of 400 μg mL^{-1}. Similar trends have been observed in all the MXenes investigated, irrespective of their etching approach or the number of layers present in the 2D material [121–123]. Thus, among the 2D materials, MXenes possess maximum application potentials with the least toxic ability.

4.3. Toxicity of chalcogenides

Among the various chalcogenides, 2D transition metal dichalcogenides (TMDs) have been extensively studied in recent years. Among these, there are three TMDs whose *in vitro* evaluations have been extensively studied: MoS_2, WS_2 and WSe_2 [124]. Generally, the MoS_2 nanomaterials of the TDG group have been studied most. Their biocompatibility was further studied on the cell lines CCC-ESF-1 (human embryonic epidermal fibroblasts), A549 (lung adenocarcinoma cells) and K562 (leukaemia cells) [125]. After treating the cells with a maximum concentration of 3.52 mg of substance 1 for 48 hours, the particles' administration did not significantly affect the CCC-ESF-1 cell line's growth. However, the study showed that the application of 3.52 mg/l of MoS_2 particles alone caused about 10% of cell death, thus demonstrating high toxic potential within.

Among the different TMDs, the ones with S, Te, Po, or Se are the most commonly available. Upon decomposition, the chalcogenides release free Te or Se elements, responsible for high toxic effects within the human body and in the environment [126,127]. When present in high concentrations, Se is known to cause high incidents of hair loss, blindness and premature deaths in animals [128]. Likewise, acute Te exposure causes suppression of salivary and sebaceous glands in humans, along with paralysis of the

secretory nerves and a high incidence rate of somnolence [129]. Furthermore, exposure to either of these two elements containing chalcogenides can result in the displacement of sulfur atoms in the proteins and peptides [130]. In addition, during the development of Te or Se based 2D materials, poisonous gas like H_2Se or H_2Te are released that harms the environment and plant and animal life alike [131].

Apart from the material's chemical composition, it also shows that the exfoliation method can significantly change TMD materials' behaviour *in vitro* and *in vivo* and their toxic potentials. For example, compared with the aggregation of MoS_2 (Agg-MoS_2), its exfoliated lithographic printing plate (Lit-MoS_2) and Pluronic F87 (PF87-MoS_2) distributed MoS_2, which has severe inflammation and pro-fibrosis effects on cells [132]. However, compared to Agg-MoS_2, 2D-MoS_2 nanomaterials are safer in lung injury. Furthermore, in another study, Yin and coworkers replaced MoS surface with chitosan, enhancing biocompatibility. As a result, a decrease was observed in the two types of cell lines KB (human epithelial cancer cell line) and Panc-1 (derived cell line) [133]. Overall, these *in vitro* results indicate that the surface modification of two-dimensional nanosheets can significantly reduce these 2D materials' toxicity and be safely used in biomedical applications.

4.4. Toxicity of 2D-oxides

Many 2D oxides are highly reactive and possess toxic properties, especially when they are present as nanoparticles. This is because they demonstrate enhanced catalytic function and high dissolution rates when the size of the 2D metal oxide decreases. For instance, V_2O_5 is a 2D metal oxide with considerable toxic potential and is commonly known as a highly poisonous chemical [134]. This 2D material is released in large quantities even during natural events of volcanic eruption and forest fires that can cause significant harm to the environment and is also known to cause genotoxicity [135]. In a study by Uche *et al*. it was observed that exposure to V_2O_5 also destroys the liver and testes of guinea pigs and also disrupt mice development stage [136].

Likewise, another 2D oxide material like MoO_3 also demonstrates severe toxic properties. Though this 2D material is used to develop other 2D materials like MoS_2, it is also known to harm human and animal life. For example, MoO_3 solids, when ingested at doses of 1.2-6 grams, have been shown to cause death in guinea pigs and rats [131]. However, this toxicity is observed only when it is present in solid form and when available in gaseous form, MoO_3 does not lead to any fatality.

Studies have also demonstrated that elements like copper oxide nanoparticles (CuO NPs) also show toxic traits in multiple cell lines. This was seen in the work by Morris *et al*., who showed that the diameter of these nanoparticles causes serum sensitive toxicity in human bronchial epithelial cell lines Beas-2B cells

[137]. The authors recorded that CuO NPs function as an irritant, and in the presence of serum, the Beas-2B cells experience squamous differentiation. Furthermore, the researchers studied the cellular uptake of varying size of CuO NPs and observed that the hydrodynamic diameter reduces when more serum is added to the cell culture. Furthermore, they also observed that the serum enhances the overall cell area and results in dose-dependent toxicity in CuO NPs with larger diameters. Therefore, this study showed that the size of CuO NPs and the serum levels in cell culture affects the functionality of Beas-2B cells. This means that multiple factors influence the toxicity of CuO NPs that including the diameter, morphology, functionalization, and concentration of the NPs, among others [138]. Studies also demonstrate that surface coatings on nanoparticles also play a crucial role in their toxicity. For instance, chitosan coating of copper nanoparticles has been shown to reduce the effects of *in vitro* toxicity and results in an inflammatory response in lung cells [139]. Thus, further research on the physical and chemical parameters of nanoparticles, including the dissolution factor, surface modifications, and exposure routes, will help better understand and minimise 2D nanomaterial toxicity [140].

Table 1 below discusses the synthetic methods, characterization techniques, applications, and toxicity of different 2-D materials.

2D Materials	Toxicity	References
Graphene	Cause dose-dependent toxicity in cells and tissues. These include lowered cell viability, apoptosis, kidney and liver tissue damage, cause lung granuloma formation	[141–143]
CuS, CuSe, $Cu_{2-x}S$, $Cu_{2-x}Se$	Damage liver cells, accumulate reactive oxygen species, cause apoptosis	[144]
$CuInS_2$, $CuIn_xGa_{1-x}S_2$, Cu_2ZnSnS_4	Severe heptatotoxicity	[145]
Au@Ag	Could be taken up by the cells and increase the overall toxicity of the cells	[146,147]
ZnSe, ZnS	Cytotoxicity, ROS production,	[148,149]

	damage to liver and brain tissues, apoptosis	
Rh	Low cytotoxicity	[150,151]
CdS	Increase in ROS species, morphological changes, biochemical disorders, neurotoxicity, pulmonary toxicity	[152–155]
Co_9Se_8	Low cytotoxicity and absorbance, biocompatibility	[156,157]
β-$Co(OH)_2$	Low toxicity	[158,159]
MoSSe	Easily adsorbs toxic gases	[160,161]
MoS_2 nanosheets	Toxicity against beneficial soil bacteria, cytotoxicity, cellular uptake, inflammatory responses	[33,162–165]
MoS_2 crystal	Induce oxidative stress, disrupt biological membrane or DNA damage	[165,166]
α-MoO_3	Low toxicity, antibacterial activity	[167,168]
α-Fe_2O_3	Antibacterial activity, induce oxidative stress, DNA damage	[169–172]
NiO	Induce ROS production, DNA damage, cytotoxicity	[173–175]
ZnO_2	Lung inflammation, systemic toxicity, oxidative stress	[176–178]
Co_3O_4	Cytotoxicity, pulmonary damage, DNA damage, oxidative stress, environmental toxicity	[179–181]
WO_3	Liver damage, apoptosis	[182,183]
TiO_2–Ga_2O_3	Relatively non-toxic	[184–187]

Journal Pre-proof

ZnO@TiO_2 nanorods	Cytoxicity, ROS production	[188–190]

Table 1: Toxicity of 2-D materials.

5. Conclusion and future prospective

Over the past couple of decades, scientists have explored tremendous advancements in synthesis, characterization, and development of various verities of advanced 2D materials for promising potential applications in diverse fields. However, complete control over the morphology of different 2D materials is required to reach their optimal activity. These 2D materials play a diverse role in packaging, sensing, automation, energy production, energy storage, electronic devices, drug delivery, orthopedic applications, biochemical sensing, among many other applications. As discussed in this review, there is a vast array of preparative processes for 2D materials, each of which has its own unique set of advantages and limitations. Hence, suitable methodologies must be employed that can be adjusted based on their target application and respective composition. Apart from their toxicity concerns, one of the significant aspects that need to be addressed immediately is their nanosafety while being handled. Most 2D materials are capable of causing biological and environmental toxicity. External conditions like ionic strength, temperature, and changes that these materials undergo inside the body affect their toxic conditions. Many surfactants used to monitor the diameter and morphology of the 2D materials during their production also contribute towards their poisonous traits. Hence, alternatives to the presently utilized surfactants will have to be considered to confer better functionality and lesser toxicity to the 2D materials. Factors like their stability within cells and their capacity to degrade and expel from the body also have to be considered to understand 2D material toxicity.

Other analytical processes need to be carried out to evaluate the real-time, in-situ regulation to enhance 2D material production efficiency. Moreover, this way, their expense, impurities, and mechanistic details can also be regulated. The main aim of nanotoxicology is to promote reproducible and relevant biosafe research and introduce precise toxicity biomarkers. Scientists also agree that there must be a dual approach to understanding 2D material toxicity before their implementation – understanding human and environmental toxicologies. There has been a vast outcry in the scientific field for investing in nanotechnology's development and furthering in recent years. There are various resultant engineered nanostructures and processes because of nanotechnology. However, further work is required to enhance the design and production of better nanomaterials. Knowledge on the size, shape and further aggregation studies because of their toxic potential is still needed to make this technology completely dependable.

Moreover, their characterization methods must be further developed and carefully realized to broaden their usage. Specific protocols must be set to study separate NPs to understand the complete toxic potential and adverse effects of the particular nanomaterial. Further studies need to be carried out to create 2D materials that are environmentally safe to be used in therapeutic and diagnostic applications.

Acknowledgement

G. A. Naikoo, Israr U. Hassan acknowledge the support received from the research council of Oman.

Author contributions: All authors have contributed equally.

Funding: NA

Availability of data and material

All data is given in the manuscript.

Competing Interests

There are no conflicts of interest to declare.

Journal Pre-proof

References:

[1] V. Kumar, N. Sharma, S.S. Maitra, In vitro and in vivo toxicity assessment of nanoparticles, Int. Nano Lett. (2017). https://doi.org/10.1007/s40089-017-0221-3.

[2] J. Jeevanandam, A. Barhoum, Y.S. Chan, A. Dufresne, M.K. Danquah, Review on nanoparticles and nanostructured materials: History, sources, toxicity and regulations, Beilstein J. Nanotechnol. (2018). https://doi.org/10.3762/bjnano.9.98.

[3] M.A. Raza, Z. Kanwal, A. Rauf, A.N. Sabri, S. Riaz, S. Naseem, Size- and shape-dependent antibacterial studies of silver nanoparticles synthesized by wet chemical routes, Nanomaterials. (2016). https://doi.org/10.3390/nano6040074.

[4] A.B. Seabra, N. Durán, Nanotoxicology of metal oxide nanoparticles, Metals (Basel). (2015). https://doi.org/10.3390/met5020934.

[5] K. Subramani, A. Elhissi, U. Subbiah, W. Ahmed, Introduction to nanotechnology, in: Nanobiomaterials Clin. Dent., 2019. https://doi.org/10.1016/B978-0-12-815886-9.00001-2.

[6] N. Mounet, M. Gibertini, P. Schwaller, D. Campi, A. Merkys, A. Marrazzo, T. Sohier, I.E. Castelli, A. Cepellotti, G. Pizzi, N. Marzari, Two-dimensional materials from high-throughput computational exfoliation of experimentally known compounds, Nat. Nanotechnol. (2018). https://doi.org/10.1038/s41565-017-0035-5.

[7] A.T. Smith, A.M. LaChance, S. Zeng, B. Liu, L. Sun, Synthesis, properties, and applications of graphene oxide/reduced graphene oxide and their nanocomposites, Nano Mater. Sci. (2019). https://doi.org/10.1016/j.nanoms.2019.02.004.

[8] J.H. Kim, T.V. Pham, J.H. Hwang, C.S. Kim, M.J. Kim, Boron nitride nanotubes: synthesis and applications, Nano Converg. (2018). https://doi.org/10.1186/s40580-018-0149-y.

[9] Z. Wei, Q. Wang, L. Li, R. Yang, G. Zhang, Monolayer MoS2 epitaxy, Nano Res. (2021). https://doi.org/10.1007/s12274-020-3019-y.

[10] C. Lee, X. Wei, J.W. Kysar, J. Hone, Measurement of the elastic properties and intrinsic strength of monolayer graphene, Science (80-.). (2008). https://doi.org/10.1126/science.1157996.

[11] N.K. Mahanta, A.R. Abramson, Thermal conductivity of graphene and graphene oxide nanoplatelets, in: Intersoc. Conf. Therm. Thermomechanical Phenom. Electron. Syst. ITHERM, 2012. https://doi.org/10.1109/ITHERM.2012.6231405.

[12] D. Legrand, L.O. Le Cunff, A. Bruyant, R. Salas-Montiel, Z. Liu, B.K. Tay, T. Maurer, R. Bachelot, Surface plasmons in suspended graphene: launching with in-plane gold nanoantenna and propagation properties, Opt. Express. (2017). https://doi.org/10.1364/oe.25.017306.

[13] T. Fang, X. Gao, X. Wang, J. Liu, Design of gate-tunable graphene electro-optical reflectors based on an optical slot-antenna coupled cavity, JPhys Photonics. (2021). https://doi.org/10.1088/2515-7647/ac266a.

[14] Y. Wu, Y.M. Lin, A.A. Bol, K.A. Jenkins, F. Xia, D.B. Farmer, Y. Zhu, P. Avouris, High-frequency, scaled graphene transistors on diamond-like carbon, Nature. (2011). https://doi.org/10.1038/nature09979.

[15] M. Alaloul, J.B. Khurgin, Plasmonic Photovoltaic Double-Graphene Detector Integrated into TiN Slot Waveguides, IEEE Photonics J. (2021). https://doi.org/10.1109/JPHOT.2021.3122105.

[16] Y. Fang, Y. Ge, C. Wang, H. Zhang, Mid-Infrared Photonics Using 2D Materials: Status and Challenges, Laser Photonics Rev. (2020). https://doi.org/10.1002/lpor.201900098.

Journal Pre-proof

[17] H. Kim, K.Y. Park, J. Hong, K. Kang, All-graphene-battery: Bridging the gap between supercapacitors and lithium ion batteries, Sci. Rep. (2014). https://doi.org/10.1038/srep05278.

[18] H.-H. Chang, T.-H. Ho, Y.-S. Su, Graphene-Enhanced Battery Components in Rechargeable Lithium-Ion and Lithium Metal Batteries, C. (2021). https://doi.org/10.3390/c7030065.

[19] X. Tang, M. Debliquy, D. Lahem, Y. Yan, J.P. Raskin, A review on functionalized graphene sensors for detection of ammonia, Sensors. (2021). https://doi.org/10.3390/s21041443.

[20] S. Sattari, M. Adeli, S. Beyranvand, M. Nemati, Functionalized graphene platforms for anticancer drug delivery, Int. J. Nanomedicine. (2021). https://doi.org/10.2147/IJN.S249712.

[21] H. Liu, A.T. Neal, Z. Zhu, Z. Luo, X. Xu, D. Tománek, P.D. Ye, Phosphorene: An unexplored 2D semiconductor with a high hole mobility, ACS Nano. (2014). https://doi.org/10.1021/nn501226z.

[22] M.A. Stoeckel, M. Gobbi, T. Leydecker, Y. Wang, M. Eredia, S. Bonacchi, R. Verucchi, M. Timpel, M.V. Nardi, E. Orgiu, P. Samorì, Boosting and Balancing Electron and Hole Mobility in Single- A nd Bilayer WSe2 Devices via Tailored Molecular Functionalization, ACS Nano. (2019). https://doi.org/10.1021/acsnano.9b05423.

[23] S. Pak, S. Jang, T. Kim, J. Lim, J.S. Hwang, Y. Cho, H. Chang, A.R. Jang, K.H. Park, J. Hong, S.N. Cha, Electrode-Induced Self-Healed Monolayer MoS2 for High Performance Transistors and Phototransistors, Adv. Mater. (2021). https://doi.org/10.1002/adma.202102091.

[24] K. Watanabe, T. Taniguchi, H. Kanda, Direct-bandgap properties and evidence for ultraviolet lasing of hexagonal boron nitride single crystal, Nat. Mater. (2004). https://doi.org/10.1038/nmat1134.

[25] Q. Ji, C. Li, J. Wang, J. Niu, Y. Gong, Z. Zhang, Q. Fang, Y. Zhang, J. Shi, L. Liao, X. Wu, L. Gu, Z. Liu, Y. Zhang, Metallic vanadium disulfide nanosheets as a platform material for multifunctional electrode applications, Nano Lett. (2017). https://doi.org/10.1021/acs.nanolett.7b01914.

[26] A.J. Mannix, Z. Zhang, N.P. Guisinger, B.I. Yakobson, M.C. Hersam, Borophene as a prototype for synthetic 2D materials development, Nat. Nanotechnol. (2018). https://doi.org/10.1038/s41565-018-0157-4.

[27] J. Wang, Y. Xu, S.C. Zhang, Two-dimensional time-reversal-invariant topological superconductivity in a doped quantum spin-Hall insulator, Phys. Rev. B - Condens. Matter Mater.

Journal Pre-proof

Phys. (2014). https://doi.org/10.1103/PhysRevB.90.054503.

[28] T. Hu, X. Mei, Y. Wang, X. Weng, R. Liang, M. Wei, Two-dimensional nanomaterials: fascinating materials in biomedical field, Sci. Bull. (2019). https://doi.org/10.1016/j.scib.2019.09.021.

[29] X. Li, J. Wang, One-dimensional and two-dimensional synergized nanostructures for high-performing energy storage and conversion, InfoMat. (2020). https://doi.org/10.1002/inf2.12040.

[30] H. Huang, Y. Cui, Q. Li, C. Dun, W. Zhou, W. Huang, L. Chen, C.A. Hewitt, D.L. Carroll, Metallic 1T phase MoS2 nanosheets for high-performance thermoelectric energy harvesting, Nano Energy. (2016). https://doi.org/10.1016/j.nanoen.2016.05.022.

[31] A.M. Jastrzębska, P. Kurtycz, A.R. Olszyna, Recent advances in graphene family materials toxicity investigations, J. Nanoparticle Res. (2012). https://doi.org/10.1007/s11051-012-1320-8.

[32] H. Lin, Z. Song, A. Bianco, How macrophages respond to two-dimensional materials: a critical overview focusing on toxicity, J. Environ. Sci. Heal. - Part B Pestic. Food Contam. Agric. Wastes. (2021). https://doi.org/10.1080/03601234.2021.1885262.

[33] E. Tan, B.L. Li, K. Ariga, C.T. Lim, S. Garaj, D.T. Leong, Toxicity of Two-Dimensional Layered Materials and Their Heterostructures, Bioconjug. Chem. (2019). https://doi.org/10.1021/acs.bioconjchem.9b00502.

[34] R. Vinoth, S.G. Babu, V. Bharti, V. Gupta, M. Navaneethan, S.V. Bhat, C. Muthamizhchelvan, P.C. Ramamurthy, C. Sharma, D.K. Aswal, Y. Hayakawa, B. Neppolian, Ruthenium based metallopolymer grafted reduced graphene oxide as a new hybrid solar light harvester in polymer solar cells, Sci. Rep. (2017). https://doi.org/10.1038/srep43133.

[35] R.K. Yadav, J.O. Lee, A. Kumar, N.J. Park, D. Yadav, J.Y. Kim, J.O. Baeg, Highly Improved Solar Energy Harvesting for Fuel Production from CO2 by a Newly Designed Graphene Film Photocatalyst, Sci. Rep. (2018). https://doi.org/10.1038/s41598-018-35135-7.

[36] K. Krishnamoorthy, P. Pazhamalai, V.K. Mariappan, S.S. Nardekar, S. Sahoo, S.J. Kim, Probing the energy conversion process in piezoelectric-driven electrochemical self-charging supercapacitor power cell using piezoelectrochemical spectroscopy, Nat. Commun. (2020). https://doi.org/10.1038/s41467-020-15808-6.

[37] S. Shimizu, J. Shiogai, N. Takemori, S. Sakai, H. Ikeda, R. Arita, T. Nojima, A. Tsukazaki, Y.

Journal Pre-proof

Iwasa, Giant thermoelectric power factor in ultrathin FeSe superconductor, Nat. Commun. (2019). https://doi.org/10.1038/s41467-019-08784-z.

[38] J.H. Meng, X. Liu, X.W. Zhang, Y. Zhang, H.L. Wang, Z.G. Yin, Y.Z. Zhang, H. Liu, J.B. You, H. Yan, Interface engineering for highly efficient graphene-on-silicon Schottky junction solar cells by introducing a hexagonal boron nitride interlayer, Nano Energy. (2016). https://doi.org/10.1016/j.nanoen.2016.08.028.

[39] Z. Yan, X. He, L. She, J. Sun, R. Jiang, H. Xu, F. Shi, Z. Lei, Z.H. Liu, Solvothermal-assisted liquid-phase exfoliation of large size and high quality black phosphorus, J. Mater. (2018). https://doi.org/10.1016/j.jmat.2018.01.003.

[40] R.S. Edwards, K.S. Coleman, Graphene film growth on polycrystalline metals, Acc. Chem. Res. (2013). https://doi.org/10.1021/ar3001266.

[41] A.V. Rane, K. Kanny, V.K. Abitha, S. Thomas, Methods for Synthesis of Nanoparticles and Fabrication of Nanocomposites, in: Synth. Inorg. Nanomater., 2018. https://doi.org/10.1016/b978-0-08-101975-7.00005-1.

[42] A.C. Pierre, Introduction to Sol-Gel Processing, 2020. https://doi.org/10.1007/978-3-030-38144-8.

[43] A.J. Expósito, D.A. Patterson, W.S.W. Mansor, J.M. Monteagudo, E. Emanuelsson, I. Sanmartín, A. Durán, Antipyrine removal by TiO2 photocatalysis based on spinning disc reactor technology, J. Environ. Manage. (2017). https://doi.org/10.1016/j.jenvman.2016.11.012.

[44] I. Khan, K. Saeed, I. Khan, Nanoparticles: Properties, applications and toxicities, Arab. J. Chem. (2019). https://doi.org/10.1016/j.arabjc.2017.05.011.

[45] R. Koirala, S.E. Pratsinis, A. Baiker, Synthesis of catalytic materials in flames: Opportunities and challenges, Chem. Soc. Rev. (2016). https://doi.org/10.1039/c5cs00011d.

[46] M. Bilal, T. Rasheed, H.M.N. Iqbal, H. Hu, X. Zhang, Silver nanoparticles: Biosynthesis and antimicrobial potentialities, Int. J. Pharmacol. (2017). https://doi.org/10.3923/ijp.2017.832.845.

[47] J. Zhang, X. Zhu, M. Wang, B. Hu, Establishing charge-transfer excitons in 2D perovskite heterostructures, Nat. Commun. (2020). https://doi.org/10.1038/s41467-020-16415-1.

[48] J.W. Lee, Z. Dai, T.H. Han, C. Choi, S.Y. Chang, S.J. Lee, N. De Marco, H. Zhao, P. Sun, Y. Huang, Y. Yang, 2D perovskite stabilized phase-pure formamidinium perovskite solar cells, Nat.

Journal Pre-proof

Commun. (2018). https://doi.org/10.1038/s41467-018-05454-4.

[49] S. Su, S. Chen, C. Fan, Recent advances in two-dimensional nanomaterials-based electrochemical sensors for environmental analysis, Green Energy Environ. (2018). https://doi.org/10.1016/j.gee.2017.08.005.

[50] Z. Wang, B. Mi, Environmental Applications of 2D Molybdenum Disulfide (MoS2) Nanosheets, Environ. Sci. Technol. (2017). https://doi.org/10.1021/acs.est.7b01466.

[51] K. Chen, B.B. Rajeeva, Z. Wu, M. Rukavina, T.D. Dao, S. Ishii, M. Aono, T. Nagao, Y. Zheng, Moiré Nanosphere Lithography, ACS Nano. (2015). https://doi.org/10.1021/acsnano.5b00978.

[52] M. Fernández-Arias, M. Boutinguiza, J. del Val, E. Medina, D. Rodríguez, A. Riveiro, R. Comesaña, F. Lusquiños, F.J. Gil, J. Pou, RE-irradiation of silver nanoparticles obtained by laser ablation in water and assessment of their antibacterial effect, Appl. Surf. Sci. (2019). https://doi.org/10.1016/j.apsusc.2018.12.182.

[53] V.J.M. Lackner, L. Major, M. Kot, W. Waldhauser, B. Major, Deformation mechanism in Ti-TiN multilayers under tribological conditions, Galvanotechnik. (2013).

[54] M. Devaraj, R. Saravanan, R. Deivasigamani, V.K. Gupta, F. Gracia, S. Jayadevan, Fabrication of novel shape Cu and Cu/Cu2O nanoparticles modified electrode for the determination of dopamine and paracetamol, J. Mol. Liq. (2016). https://doi.org/10.1016/j.molliq.2016.06.028.

[55] S. Fan, R. Cao, L. Wang, S. Gao, Y. Zhang, X. Yu, H. Zhang, Quantum tunneling in two-dimensional van der Waals heterostructures and devices, Sci. China Mater. (2021). https://doi.org/10.1007/s40843-021-1685-y.

[56] J.N. Coleman, M. Lotya, A. O'Neill, S.D. Bergin, P.J. King, U. Khan, K. Young, A. Gaucher, S. De, R.J. Smith, I. V. Shvets, S.K. Arora, G. Stanton, H.Y. Kim, K. Lee, G.T. Kim, G.S. Duesberg, T. Hallam, J.J. Boland, J.J. Wang, J.F. Donegan, J.C. Grunlan, G. Moriarty, A. Shmeliov, R.J. Nicholls, J.M. Perkins, E.M. Grieveson, K. Theuwissen, D.W. McComb, P.D. Nellist, V. Nicolosi, Two-dimensional nanosheets produced by liquid exfoliation of layered materials, Science (80-.). (2011). https://doi.org/10.1126/science.1194975.

[57] J. Kang, J.W.T. Seo, D. Alducin, A. Ponce, M.J. Yacaman, M.C. Hersam, Thickness sorting of two-dimensional transition metal dichalcogenides via copolymer-assisted density gradient ultracentrifugation, Nat. Commun. (2014). https://doi.org/10.1038/ncomms6478.

Journal Pre-proof

[58] S. Xu, Z. Yan, K.I. Jang, W. Huang, H. Fu, J. Kim, Z. Wei, M. Flavin, J. McCracken, R. Wang, A. Badea, Y. Liu, D. Xiao, G. Zhou, J. Lee, H.U. Chung, H. Cheng, W. Ren, A. Banks, X. Li, U. Paik, R.G. Nuzzo, Y. Huang, Y. Zhang, J.A. Rogers, Assembly of micro/nanomaterials into complex, three-dimensional architectures by compressive buckling, Science (80-.). (2015). https://doi.org/10.1126/science.1260960.

[59] A. Rockett, The materials science of semiconductors, 2008. https://doi.org/10.1007/978-0-387-68650-9.

[60] X. Li, W. Cai, J. An, S. Kim, J. Nah, D. Yang, R. Piner, A. Velamakanni, I. Jung, E. Tutuc, S.K. Banerjee, L. Colombo, R.S. Ruoff, Large-area synthesis of high-quality and uniform graphene films on copper foils, Science (80-.). (2009). https://doi.org/10.1126/science.1171245.

[61] J.H. Lee, E.K. Lee, W.J. Joo, Y. Jang, B.S. Kim, J.Y. Lim, S.H. Choi, S.J. Ahn, J.R. Ahn, M.H. Park, C.W. Yang, B.L. Choi, S.W. Hwang, D. Whang, Wafer-scale growth of single-crystal monolayer graphene on reusable hydrogen-terminated germanium, Science (80-.). (2014). https://doi.org/10.1126/science.1252268.

[62] G.M. Rutter, J.N. Crain, N.P. Guisinger, T. Li, P.N. First, J.A. Stroscio, Scattering and interference in epitaxial graphene, Science (80-.). (2007). https://doi.org/10.1126/science.1142882.

[63] C. Backes, A.M. Abdelkader, C. Alonso, A. Andrieux-Ledier, R. Arenal, J. Azpeitia, N. Balakrishnan, L. Banszerus, J. Barjon, R. Bartali, S. Bellani, C. Berger, R. Berger, M.M.B. Ortega, C. Bernard, P.H. Beton, A. Beyer, A. Bianco, P. Bøggild, F. Bonaccorso, G.B. Barin, C. Botas, R.A. Bueno, D. Carriazo, A. Castellanos-Gomez, M. Christian, A. Ciesielski, T. Ciuk, M.T. Cole, J. Coleman, C. Coletti, L. Crema, H. Cun, D. Dasler, D. De Fazio, N. Díez, S. Drieschner, G.S. Duesberg, R. Fasel, X. Feng, A. Fina, S. Forti, C. Galiotis, G. Garberoglio, J.M. García, J.A. Garrido, M. Gibertini, A. Gölzhäuser, J. Gómez, T. Greber, F. Hauke, A. Hemmi, I. Hernandez-Rodriguez, A. Hirsch, S.A. Hodge, Y. Huttel, P.U. Jepsen, I. Jimenez, U. Kaiser, T. Kaplas, H.K. Kim, A. Kis, K. Papagelis, K. Kostarelos, A. Krajewska, K. Lee, C. Li, H. Lipsanen, A. Liscio, M.R. Lohe, A. Loiseau, L. Lombardi, M.F. López, O. Martin, C. Martín, L. Martínez, J.A. Martin-Gago, J.I. Martínez, N. Marzari, Á. Mayoral, J. McManus, M. Melucci, J. Méndez, C. Merino, P. Merino, A.P. Meyer, E. Miniussi, V. Miseikis, N. Mishra, V. Morandi, C. Munuera, R. Muñoz, H. Nolan, L. Ortolani, A.K. Ott, I. Palacio, V. Palermo, J. Parthenios, I. Pasternak, A. Patane, M. Prato, H. Prevost, V. Prudkovskiy, N. Pugno, T. Rojo, A. Rossi, P. Ruffieux, P. Samorì, L. Schué,

E. Setijadi, T. Seyller, G. Speranza, C. Stampfer, I. Stenger, W. Strupinski, Y. Svirko, S. Taioli, K.B.K. Teo, M. Testi, F. Tomarchio, M. Tortello, E. Treossi, A. Turchanin, E. Vazquez, E. Villaro, P.R. Whelan, Z. Xia, R. Yakimova, S. Yang, G.R. Yazdi, C. Yim, D. Yoon, X. Zhang, X. Zhuang, L. Colombo, A.C. Ferrari, M. Garcia-Hernandez, Production and processing of graphene and related materials, 2D Mater. (2020). https://doi.org/10.1088/2053-1583/ab1e0a.

[64] Q. Wu, W. Wongwiriyapan, J.H. Park, S. Park, S.J. Jung, T. Jeong, S. Lee, Y.H. Lee, Y.J. Song, In situ chemical vapor deposition of graphene and hexagonal boron nitride heterostructures, Curr. Appl. Phys. (2016). https://doi.org/10.1016/j.cap.2016.04.024.

[65] R.R. Poolakkandy, M.M. Menamparambath, Soft-template-assisted synthesis: A promising approach for the fabrication of transition metal oxides, Nanoscale Adv. (2020). https://doi.org/10.1039/d0na00599a.

[66] S. Yi, F. Dai, C. Zhao, Y. Si, A reverse micelle strategy for fabricating magnetic lipase-immobilized nanoparticles with robust enzymatic activity, Sci. Rep. (2017). https://doi.org/10.1038/s41598-017-10453-4.

[67] N. Pugazhenthiran, R. V. Mangalaraja, P. Sathishkumar, S. Murugesan, T. Muneeswaran, T. Pandiyarajan, S. Naveenraj, D. Contreras, S. Anandan, Green synthesis of porous Au-Nx-TiO2 nanospheres for solar light induced photocatalytic degradation of diazo and triazo dyes and their eco-toxic effects, New J. Chem. (2018). https://doi.org/10.1039/c8nj04554b.

[68] L. Lu, C. Zhang, B. Zou, Y. Wang, Hollow prussian blue nanospheres for photothermal/chemo-synergistic therapy, Int. J. Nanomedicine. (2020). https://doi.org/10.2147/IJN.S252505.

[69] Z. Zhang, H.C. Schniepp, D.H. Adamson, Characterization of graphene oxide: Variations in reported approaches, Carbon N. Y. (2019). https://doi.org/10.1016/j.carbon.2019.07.103.

[70] P.R. Whelan, B. Zhou, O. Bezencenet, A. Shivayogimath, N. Mishra, Q. Shen, B.S. Jessen, I. Pasternak, D.M.A. Mackenzie, J. Ji, C. Sun, P. Seneor, B. Dlubak, B. Luo, F.W. Østerberg, D. Huang, H. Shi, D. Luo, M. Wang, R.S. Ruoff, B.R. Conran, C. McAleese, C. Huyghebaert, S. Brems, T.J. Booth, I. Napal, W. Strupinski, D.H. Petersen, S. Forti, C. Coletti, A. Jouvray, K.B.K. Teo, A. Centeno, A. Zurutuza, P. Legagneux, P.U. Jepsen, P. Bøggild, Case studies of electrical characterisation of graphene by terahertz time-domain spectroscopy, 2D Mater. (2021). https://doi.org/10.1088/2053-1583/abdbcb.

[71] J. Bin Wu, M.L. Lin, X. Cong, H.N. Liu, P.H. Tan, Raman spectroscopy of graphene-based

Journal Pre-proof

materials and its applications in related devices, Chem. Soc. Rev. (2018). https://doi.org/10.1039/c6cs00915h.

[72] H. Xu, X. Wu, X. Li, C. Luo, F. Liang, E. Orignac, J. Zhang, J. Chu, Properties of graphene-metal contacts probed by Raman spectroscopy, Carbon N. Y. (2018). https://doi.org/10.1016/j.carbon.2017.11.035.

[73] J. Overbeck, G. Borin Barin, C. Daniels, M.L. Perrin, L. Liang, O. Braun, R. Darawish, B. Burkhardt, T. Dumslaff, X.Y. Wang, A. Narita, K. Müllen, V. Meunier, R. Fasel, M. Calame, P. Ruffieux, Optimized Substrates and Measurement Approaches for Raman Spectroscopy of Graphene Nanoribbons, Phys. Status Solidi Basic Res. (2019). https://doi.org/10.1002/pssb.201900343.

[74] A.C. Ferrari, Raman spectroscopy of graphene and graphite: Disorder, electron-phonon coupling, doping and nonadiabatic effects, Solid State Commun. (2007). https://doi.org/10.1016/j.ssc.2007.03.052.

[75] W.W. Liu, S.P. Chai, A.R. Mohamed, U. Hashim, Synthesis and characterization of graphene and carbon nanotubes: A review on the past and recent developments, J. Ind. Eng. Chem. (2014). https://doi.org/10.1016/j.jiec.2013.08.028.

[76] X. Li, Z.Y. Xin, J.S. Li, Growth of graphene from solid carbon sources, in: Text. Bioeng. Informatics Symp. Proc. 2018 - 11th Text. Bioeng. Informatics Symp. TBIS 2018, 2018.

[77] R. Farzana, R. Rajarao, P.R. Behera, K. Hassan, V. Sahajwalla, Zinc oxide nanoparticles from waste Zn-C battery via thermal route: Characterization and properties, Nanomaterials. (2018). https://doi.org/10.3390/nano8090717.

[78] V. Garg, R.G. Mote, J. Fu, Facile fabrication of functional 3D micro-nano architectures with focused ion beam implantation and selective chemical etching, Appl. Surf. Sci. (2020). https://doi.org/10.1016/j.apsusc.2020.146644.

[79] H.H. Son, G.H. Seo, U. Jeong, D.Y. Shin, S.J. Kim, Capillary wicking effect of a Cr-sputtered superhydrophilic surface on enhancement of pool boiling critical heat flux, Int. J. Heat Mass Transf. (2017). https://doi.org/10.1016/j.ijheatmasstransfer.2017.05.055.

[80] M. Shekhirev, C.E. Shuck, A. Sarycheva, Y. Gogotsi, Characterization of MXenes at every step, from their precursors to single flakes and assembled films, Prog. Mater. Sci. (2021).

Journal Pre-proof

https://doi.org/10.1016/j.pmatsci.2020.100757.

[81] X. Mu, D. Wang, F. Du, G. Chen, C. Wang, Y. Wei, Y. Gogotsi, Y. Gao, Y. Dall'Agnese, Revealing the Pseudo-Intercalation Charge Storage Mechanism of MXenes in Acidic Electrolyte, Adv. Funct. Mater. (2019). https://doi.org/10.1002/adfm.201902953.

[82] C. Shi, M. Beidaghi, M. Naguib, O. Mashtalir, Y. Gogotsi, S.J.L. Billinge, Structure of nanocrystalline Ti3 C2 MXene using atomic pair distribution function, Phys. Rev. Lett. (2013). https://doi.org/10.1103/PhysRevLett.112.125501.

[83] M. Ghidiu, M. Naguib, C. Shi, O. Mashtalir, L.M. Pan, B. Zhang, J. Yang, Y. Gogotsi, S.J.L. Billinge, M.W. Barsoum, Synthesis and characterization of two-dimensional Nb4C3 (MXene), Chem. Commun. (2014). https://doi.org/10.1039/c4cc03366c.

[84] H.W. Wang, M. Naguib, K. Page, D.J. Wesolowski, Y. Gogotsi, Resolving the Structure of Ti3C2Tx MXenes through Multilevel Structural Modeling of the Atomic Pair Distribution Function, Chem. Mater. (2016). https://doi.org/10.1021/acs.chemmater.5b04250.

[85] W. Sun, H.W. Wang, L. Vlcek, J. Peng, A.B. Brady, N.C. Osti, E. Mamontov, M. Tyagi, J. Nanda, S.G. Greenbaum, P.R.C. Kent, M. Naguib, Multiscale and Multimodal Characterization of 2D Titanium Carbonitride MXene, Adv. Mater. Interfaces. (2020). https://doi.org/10.1002/admi.201902207.

[86] C. Wang, S. Chen, L. Song, Tuning 2D MXenes by Surface Controlling and Interlayer Engineering: Methods, Properties, and Synchrotron Radiation Characterizations, Adv. Funct. Mater. (2020). https://doi.org/10.1002/adfm.202000869.

[87] A. Selezen, Y. Kogut, L. Piskach, L. Gulay, New Quaternary Chalcogenides Tl2MIIMIV3Se8 and Tl2MIIMIVX4, Proceedings. (2020). https://doi.org/10.3390/proceedings2020062003.

[88] S.C. Sahu, J. Zheng, L. Graham, L. Chen, J. Ihrie, J.J. Yourick, R.L. Sprando, Comparative cytotoxicity of nanosilver in human liver HepG2 and colon Caco2 cells in culture, J. Appl. Toxicol. (2014). https://doi.org/10.1002/jat.2994.

[89] C.D. Lokhande, B.R. Sankapal, R.S. Mane, H.M. Pathan, M. Muller, M. Giersig, V. Ganesan, XRD, SEM, AFM, HRTEM, EDAX and RBS studies of chemically deposited Sb 2 S 3 and Sb 2 Se 3 thin films, Appl. Surf. Sci. (2002). https://doi.org/10.1016/S0169-4332(01)00819-4.

[90] T.S. Bhat, S.S. Mali, A.D. Sheikh, N.L. Tarwal, S.D. Korade, C.K. Hong, J.H. Kim, P.S. Patil,

ZnS passivated PbSe sensitized TiO2 nanorod arrays to suppress photocorrosion in photoelectrochemical solar cells, Mater. Today Commun. (2018). https://doi.org/10.1016/j.mtcomm.2018.06.008.

[91] A. Mardyukov, F. Keul, P.R. Schreiner, Isolation and Characterization of the Free Phenylphosphinidene Chalcogenides C6H5P=O and C6H5P=S, the Phosphorous Analogues of Nitrosobenzene and Thionitrosobenzene, Angew. Chemie - Int. Ed. (2020). https://doi.org/10.1002/anie.202004172.

[92] S.B. Basuvalingam, Y. Zhang, M.A. Bloodgood, R.H. Godiksen, A.G. Curto, J.P. Hofmann, M.A. Verheijen, W.M.M. Kessels, A.A. Bol, Low-Temperature Phase-Controlled Synthesis of Titanium Di- And Tri-sulfide by Atomic Layer Deposition, Chem. Mater. (2019). https://doi.org/10.1021/acs.chemmater.9b02895.

[93] Y. Chen, Q. Li, Z. Yang, X. Shen, X. Wang, R. Wang, M. Zhang, Quantitative estimation of crystallization kinetics in GeGaS and Au-doped GeGaS glass-ceramics, J. Am. Ceram. Soc. (2020). https://doi.org/10.1111/jace.16828.

[94] J.H. Joshi, D.K. Kanchan, M.J. Joshi, H.O. Jethva, K.D. Parikh, Dielectric relaxation, complex impedance and modulus spectroscopic studies of mix phase rod like cobalt sulfide nanoparticles, Mater. Res. Bull. (2017). https://doi.org/10.1016/j.materresbull.2017.04.013.

[95] S.K. Radha, K. Crowley, B.A. Holler, X.P.A. Gao, W.R.L. Lambrecht, H. Volkova, M.H. Berger, E. Pentzer, K.G. Pachuta, A. Sehirlioglu, Ultrathin 2D-oxides: A perspective on fabrication, structure, defect, transport, electron, and phonon properties, J. Appl. Phys. (2021). https://doi.org/10.1063/5.0051093.

[96] S. Sucharitakul, G. Ye, W.R.L. Lambrecht, C. Bhandari, A. Gross, R. He, H. Poelman, X.P.A. Gao, V2O5: A 2D van der Waals Oxide with Strong In-Plane Electrical and Optical Anisotropy, ACS Appl. Mater. Interfaces. (2017). https://doi.org/10.1021/acsami.7b05377.

[97] R. Seif El-Nasr, S.M. Abdelbasir, A.H. Kamel, S.S.M. Hassan, Environmentally friendly synthesis of copper nanoparticles from waste printed circuit boards, Sep. Purif. Technol. (2020). https://doi.org/10.1016/j.seppur.2019.115860.

[98] J. Singh, T. Dutta, K.H. Kim, M. Rawat, P. Samddar, P. Kumar, “Green” synthesis of metals and their oxide nanoparticles: Applications for environmental remediation, J. Nanobiotechnology. (2018). https://doi.org/10.1186/s12951-018-0408-4.

Journal Pre-proof

[99] V. Nicolosi, M. Chhowalla, M.G. Kanatzidis, M.S. Strano, J.N. Coleman, Liquid exfoliation of layered materials, Science (80-.). (2013). https://doi.org/10.1126/science.1226419.

[100] K.H. Kim, B. Kumar, K.Y. Lee, H.K. Park, J.H. Lee, H.H. Lee, H. Jun, D. Lee, S.W. Kim, Piezoelectric two-dimensional nanosheets/anionic layer heterojunction for efficient direct current power generation, Sci. Rep. (2013). https://doi.org/10.1038/srep02017.

[101] H. Liu, Y. Feng, J. Shao, Y. Chen, Z.L. Wang, H. Li, X. Chen, Z. Bian, Self-cleaning triboelectric nanogenerator based on TiO2 photocatalysis, Nano Energy. (2020). https://doi.org/10.1016/j.nanoen.2020.104499.

[102] S. Jang, J.H. Oh, Rapid Fabrication of Microporous BaTiO3/PDMS Nanocomposites for Triboelectric Nanogenerators through One-step Microwave Irradiation, Sci. Rep. (2018). https://doi.org/10.1038/s41598-018-32609-6.

[103] J.H. Liu, S.T. Yang, H. Wang, Y. Chang, A. Cao, Y. Liu, Effect of size and dose on the biodistribution of graphene oxide in mice, Nanomedicine. (2012). https://doi.org/10.2217/nnm.12.60.

[104] B. Strojny, N. Kurantowicz, E. Sawosz, M. Grodzik, S. Jaworski, M. Kutwin, M. Wierzbicki, A. Hotowy, L. Lipińska, A. Chwalibog, Long term influence of carbon nanoparticles on health and liver status in rats, PLoS One. (2015). https://doi.org/10.1371/journal.pone.0144821.

[105] J. Dong, Q. Ma, Myofibroblasts and lung fibrosis induced by carbon nanotube exposure, Part. Fibre Toxicol. (2016). https://doi.org/10.1186/s12989-016-0172-2.

[106] X. Baur, S. Sanyal, J.L. Abraham, Mixed-dust pneumoconiosis: Review of diagnostic and classification problems with presentation of a work-related case, Sci. Total Environ. (2019). https://doi.org/10.1016/j.scitotenv.2018.10.083.

[107] X. Hu, S. Cook, P. Wang, H. min Hwang, In vitro evaluation of cytotoxicity of engineered metal oxide nanoparticles, Sci. Total Environ. (2009). https://doi.org/10.1016/j.scitotenv.2009.01.033.

[108] N. Lu, L. Wang, M. Lv, Z. Tang, C. Fan, Graphene-based nanomaterials in biosystems, Nano Res. (2019). https://doi.org/10.1007/s12274-018-2209-3.

[109] L. Ou, B. Song, H. Liang, J. Liu, X. Feng, B. Deng, T. Sun, L. Shao, Toxicity of graphene-family nanoparticles: A general review of the origins and mechanisms, Part. Fibre Toxicol. (2016). https://doi.org/10.1186/s12989-016-0168-y.

Journal Pre-proof

[110] R. Pecoraro, D. D'Angelo, S. Filice, S. Scalese, F. Capparucci, F. Marino, C. Iaria, G. Guerriero, D. Tibullo, E.M. Scalisi, A. Salvaggio, I. Nicotera, M. V. Brundo, Toxicity evaluation of graphene oxide and titania loaded nafion membranes in zebrafish, Front. Physiol. (2018). https://doi.org/10.3389/fphys.2017.01039.

[111] S. Mittal, V. Kumar, N. Dhiman, L.K.S. Chauhan, R. Pasricha, A.K. Pandey, Physico-chemical properties based differential toxicity of graphene oxide/reduced graphene oxide in human lung cells mediated through oxidative stress, Sci. Rep. (2016). https://doi.org/10.1038/srep39548.

[112] C.E. Shuck, K. Ventura-Martinez, A. Goad, S. Uzun, M. Shekhirev, Y. Gogotsi, Safe Synthesis of MAX and MXene: Guidelines to Reduce Risk During Synthesis, ACS Chem. Heal. Saf. (2021). https://doi.org/10.1021/acs.chas.1c00051.

[113] I. Ihsanullah, Potential of MXenes in Water Desalination: Current Status and Perspectives, Nano-Micro Lett. (2020). https://doi.org/10.1007/s40820-020-0411-9.

[114] M.A. Unal, F. Bayrakdar, L. Fusco, O. Besbinar, C.E. Shuck, S. Yalcin, M.T. Erken, A. Ozkul, C. Gurcan, O. Panatli, G.Y. Summak, C. Gokce, M. Orecchioni, A. Gazzi, F. Vitale, J. Somers, E. Demir, S.S. Yildiz, H. Nazir, J.C. Grivel, D. Bedognetti, A. Crisanti, K.C. Akcali, Y. Gogotsi, L.G. Delogu, A. Yilmazer, 2D MXenes with antiviral and immunomodulatory properties: A pilot study against SARS-CoV-2, Nano Today. (2021). https://doi.org/10.1016/j.nantod.2021.101136.

[115] N. Driscoll, A.G. Richardson, K. Maleski, B. Anasori, O. Adewole, P. Lelyukh, L. Escobedo, D.K. Cullen, T.H. Lucas, Y. Gogotsi, F. Vitale, Two-Dimensional Ti3C2 MXene for High-Resolution Neural Interfaces, ACS Nano. (2018). https://doi.org/10.1021/acsnano.8b06014.

[116] S. Pan, J. Yin, L. Yu, C. Zhang, Y. Zhu, Y. Gao, Y. Chen, 2D MXene-Integrated 3D-Printing Scaffolds for Augmented Osteosarcoma Phototherapy and Accelerated Tissue Reconstruction, Adv. Sci. (2020). https://doi.org/10.1002/advs.201901511.

[117] A. Rozmysłowska-Wojciechowska, A. Szuplewska, T. Wojciechowski, S. Poźniak, J. Mitrzak, M. Chudy, W. Ziemkowska, L. Chlubny, A. Olszyna, A.M. Jastrzębska, A simple, low-cost and green method for controlling the cytotoxicity of MXenes, Mater. Sci. Eng. C. (2020). https://doi.org/10.1016/j.msec.2020.110790.

[118] A.M. Jastrzębska, A. Szuplewska, T. Wojciechowski, M. Chudy, W. Ziemkowska, L. Chlubny, A. Rozmysłowska, A. Olszyna, In vitro studies on cytotoxicity of delaminated Ti3C2 MXene, J. Hazard. Mater. (2017). https://doi.org/10.1016/j.jhazmat.2017.06.004.

Journal Pre-proof

[119] X. Han, J. Huang, H. Lin, Z. Wang, P. Li, Y. Chen, 2D Ultrathin MXene-Based Drug-Delivery Nanoplatform for Synergistic Photothermal Ablation and Chemotherapy of Cancer, Adv. Healthc. Mater. (2018). https://doi.org/10.1002/adhm.201701394.

[120] G.K. Nasrallah, M. Al-Asmakh, K. Rasool, K.A. Mahmoud, Ecotoxicological assessment of Ti3C2T:X (MXene) using a zebrafish embryo model, Environ. Sci. Nano. (2018). https://doi.org/10.1039/c7en01239j.

[121] M.E. Marchwiany, M. Birowska, M. Popielski, J.A. Majewski, A.M. Jastrzebska, Surface-related features responsible for cytotoxic behavior of mxenes layered materials predicted with machine learning approach, Materials (Basel). (2020). https://doi.org/10.3390/ma13143083.

[122] A.M. Jastrzębska, A. Szuplewska, A. Rozmysłowska-Wojciechowska, M. Chudy, A. Olszyna, M. Birowska, M. Popielski, J.A. Majewski, B. Scheibe, V. Natu, M.W. Barsoum, On tuning the cytotoxicity of Ti3C2 (MXene) flakes to cancerous and benign cells by post-delamination surface modifications, 2D Mater. (2020). https://doi.org/10.1088/2053-1583/ab6a60.

[123] A. Szuplewska, A. Rozmysłowska-Wojciechowska, S. Poźniak, T. Wojciechowski, M. Birowska, M. Popielski, M. Chudy, W. Ziemkowska, L. Chlubny, D. Moszczyńska, A. Olszyna, J.A. Majewski, A.M. Jastrzębska, Multilayered stable 2D nano-sheets of Ti2NTx MXene: Synthesis, characterization, and anticancer activity, J. Nanobiotechnology. (2019). https://doi.org/10.1186/s12951-019-0545-4.

[124] W.Z. Teo, E.L.K. Chng, Z. Sofer, M. Pumera, Cytotoxicity of exfoliated transition-metal dichalcogenides (MoS 2, WS2, and WSe2) is lower than that of graphene and its analogues, Chem. - A Eur. J. (2014). https://doi.org/10.1002/chem.201402680.

[125] H. Wu, R. Yang, B. Song, Q. Han, J. Li, Y. Zhang, Y. Fang, R. Tenne, C. Wang, Biocompatible inorganic fullerene-like molybdenum disulfide nanoparticles produced by pulsed laser ablation in water, ACS Nano. (2011). https://doi.org/10.1021/nn102941b.

[126] M. Gupta, S. Gupta, An overview of selenium uptake, metabolism, and toxicity in plants, Front. Plant Sci. (2017). https://doi.org/10.3389/fpls.2016.02074.

[127] B.B. Pereira, J.E. Limongi, E.O. de Campos JÚnior, D.P. Luiz, W.E. Kerr, Effects of piperonyl butoxide on the toxicity of the organophosphate temephos and the role of esterases in the insecticide resistance of Aedes aegypti, Rev. Soc. Bras. Med. Trop. (2014). https://doi.org/10.1590/0037-8682-0195-2014.

Journal Pre-proof

[128] U. Saha, Selenium in Animal Nutrition: Deficiencies in Soils and Forages, Requirements, Supplementation and Toxicity, Int. J. Appl. Agric. Sci. (2016). https://doi.org/10.11648/j.ijaas.20160206.15.

[129] M. Nurunnabi, J.R. McCarthy, Biomedical applications of graphene and 2D nanomaterials, 2019. https://doi.org/10.1016/C2017-0-02937-3.

[130] L. Moroder, Isosteric replacement of sulfur with other chalcogens in peptides and proteins, J. Pept. Sci. (2005). https://doi.org/10.1002/psc.654.

[131] N.C.D. Nath, T. Debnath, M. Nurunnabi, E.K. Kim, In vitro toxicity of 2D materials, in: Biomed. Appl. Graphene 2D Nanomater., 2019. https://doi.org/10.1016/B978-0-12-815889-0.00008-8.

[132] X. Wang, N.D. Mansukhani, L.M. Guiney, Z. Ji, C.H. Chang, M. Wang, Y.P. Liao, T. Bin Song, B. Sun, R. Li, T. Xia, M.C. Hersam, A.E. Nel, Differences in the Toxicological Potential of 2D versus Aggregated Molybdenum Disulfide in the Lung, Small. (2015). https://doi.org/10.1002/smll.201500906.

[133] W. Yin, L. Yan, J. Yu, G. Tian, L. Zhou, X. Zheng, X. Zhang, Y. Yong, J. Li, Z. Gu, Y. Zhao, High-throughput synthesis of single-layer MoS2 nanosheets as a near-infrared photothermal-triggered drug delivery for effective cancer therapy, ACS Nano. (2014). https://doi.org/10.1021/nn501647j.

[134] S. Areecheewakul, A. Adamcakova-Dodd, B.E. Givens, B.R. Steines, Y. Wang, D.K. Meyerholz, N.J. Parizek, R. Altmaier, E. Haque, P.T. O'Shaughnessy, A.K. Salem, P.S. Thorne, Toxicity assessment of metal oxide nanomaterials using in vitro screening and murine acute inhalation studies, NanoImpact. (2020). https://doi.org/10.1016/j.impact.2020.100214.

[135] E.J. Park, G.H. Lee, C. Yoon, D.W. Kim, Comparison of distribution and toxicity following repeated oral dosing of different vanadium oxide nanoparticles in mice, Environ. Res. (2016). https://doi.org/10.1016/j.envres.2016.05.036.

[136] F. Uche, A. Obianime, M. Gogo-Abite, Effects of Vanadium Pentoxide on the Histological and Sperm Parameters of Male Guinea Pigs, J. Appl. Sci. Environ. Manag. (2010). https://doi.org/10.4314/jasem.v12i3.55512.

[137] A.S. Morris, B.E. Givens, A. Silva, A.K. Salem, Copper Oxide Nanoparticle Diameter Mediates Serum-Sensitive Toxicity in BEAS-2B Cells, Adv. NanoBiomed Res. (2021).

Journal Pre-proof

https://doi.org/10.1002/anbr.202000062.

[138] S. Naz, A. Gul, M. Zia, Toxicity of copper oxide nanoparticles: A review study, IET Nanobiotechnology. (2020). https://doi.org/10.1049/iet-nbt.2019.0176.

[139] K.L.S. Worthington, A. Adamcakova-Dodd, A. Wongrakpanich, I.A. Mudunkotuwa, K.A. Mapuskar, V.B. Joshi, C. Allan Guymon, D.R. Spitz, V.H. Grassian, P.S. Thorne, A.K. Salem, Chitosan coating of copper nanoparticles reduces in vitro toxicity and increases inflammation in the lung, Nanotechnology. (2013). https://doi.org/10.1088/0957-4484/24/39/395101.

[140] E. Sánchez-López, D. Gomes, G. Esteruelas, L. Bonilla, A.L. Lopez-Machado, R. Galindo, A. Cano, M. Espina, M. Ettcheto, A. Camins, A.M. Silva, A. Durazzo, A. Santini, M.L. Garcia, E.B. Souto, Metal-based nanoparticles as antimicrobial agents: An overview, Nanomaterials. (2020). https://doi.org/10.3390/nano10020292.

[141] R. Rajakumari, A. Tharayil, S. Thomas, N. Kalarikkal, Toxicity of graphene based nanomaterials—A general overview of origin, exposure and mechanisms, in: Compr. Anal. Chem., 2020. https://doi.org/10.1016/bs.coac.2020.09.004.

[142] A. Rhazouani, H. Gamrani, M. El Achaby, K. Aziz, L. Gebrati, M.S. Uddin, F. Aziz, Synthesis and Toxicity of Graphene Oxide Nanoparticles: A Literature Review of in Vitro and in Vivo Studies, Biomed Res. Int. (2021). https://doi.org/10.1155/2021/5518999.

[143] L. Zhang, S. Ouyang, H. Zhang, M. Qiu, Y. Dai, S. Wang, Y. Wang, J. Ou, Graphene oxide induces dose-dependent lung injury in rats by regulating autophagy, Exp. Ther. Med. (2021). https://doi.org/10.3892/etm.2021.9893.

[144] H.J. Wang, G.G. Yang, S.S. Wu, Z.F. Meng, J.M. Zhang, Y. Cao, Y.P. Zhang, Toxicity of CuS/CdS semiconductor nanocomposites to liver cells and mice liver, Sci. Total Environ. (2021). https://doi.org/10.1016/j.scitotenv.2021.147221.

[145] J.C. Kays, A.M. Saeboe, R. Toufanian, D.E. Kurant, A.M. Dennis, Shell-Free Copper Indium Sulfide Quantum Dots Induce Toxicity in Vitro and in Vivo, Nano Lett. (2020). https://doi.org/10.1021/acs.nanolett.9b05259.

[146] T.L. Botha, E.E. Elemike, S. Horn, D.C. Onwudiwe, J.P. Giesy, V. Wepener, Cytotoxicity of Ag, Au and Ag-Au bimetallic nanoparticles prepared using golden rod (Solidago canadensis) plant extract, Sci. Rep. (2019). https://doi.org/10.1038/s41598-019-40816-y.

Journal Pre-proof

[147] S.B. Yaqoob, R. Adnan, R.M. Rameez Khan, M. Rashid, Gold, Silver, and Palladium Nanoparticles: A Chemical Tool for Biomedical Applications, Front. Chem. (2020). https://doi.org/10.3389/fchem.2020.00376.

[148] R. Zhang, X. Yan, K. Fan, Nanozymes Inspired by Natural Enzymes, Accounts Mater. Res. (2021). https://doi.org/10.1021/accountsmr.1c00074.

[149] V.G. Reshma, P. V. Mohanan, Assessment of Immunotoxicity and Oxidative Stress Induced by Zinc Selenium/Zinc Sulphide Quantum Dots, Front. Nanotechnol. (2021). https://doi.org/10.3389/fnano.2020.597382.

[150] H. Duan, N. Yan, R. Yu, C.R. Chang, G. Zhou, H.S. Hu, H. Rong, Z. Niu, J. Mao, H. Asakura, T. Tanaka, P.J. Dyson, J. Li, Y. Li, Ultrathin rhodium nanosheets, Nat. Commun. (2014). https://doi.org/10.1038/ncomms4093.

[151] K.M. Boyle, J.K. Barton, A Family of Rhodium Complexes with Selective Toxicity toward Mismatch Repair-Deficient Cancers, J. Am. Chem. Soc. (2018). https://doi.org/10.1021/jacs.8b02271.

[152] S.T. Hossain, S.K. Mukherjee, Toxicity of cadmium sulfide (CdS) nanoparticles against Escherichia coli and HeLa cells, J. Hazard. Mater. (2013). https://doi.org/10.1016/j.jhazmat.2013.07.005.

[153] K. Pikula, N. Mintcheva, S.A. Kulinich, A. Zakharenko, Z. Markina, V. Chaika, T. Orlova, Y. Mezhuev, E. Kokkinakis, A. Tsatsakis, K. Golokhvast, Aquatic toxicity and mode of action of CdS and ZnS nanoparticles in four microalgae species, Environ. Res. (2020). https://doi.org/10.1016/j.envres.2020.109513.

[154] A. Varmazyari, A. Taghizadehghalehjoughi, C. Sevim, O. Baris, G. Eser, S. Yildirim, A. Hacimuftuoglu, A. Buha, D.R. Wallace, A. Tsatsakis, M. Aschner, Y. Mezhuev, Cadmium sulfide-induced toxicity in the cortex and cerebellum: In vitro and in vivo studies, Toxicol. Reports. (2020). https://doi.org/10.1016/j.toxrep.2020.04.011.

[155] J.R. Roberts, J.M. Antonini, D.W. Porter, R.S. Chapman, J.F. Scabilloni, S.H. Young, D. Schwegler-Berry, V. Castranova, R.R. Mercer, Lung toxicity and biodistribution of Cd/Se-ZnS quantum dots with different surface functional groups after pulmonary exposure in rats., Part. Fibre Toxicol. (2013). https://doi.org/10.1186/1743-8977-10-5.

Journal Pre-proof

[156] X.R. Song, X. Wang, S.X. Yu, J. Cao, S.H. Li, J. Li, G. Liu, H.H. Yang, X. Chen, Co9Se8 nanoplates as a new theranostic platform for photoacoustic/magnetic resonance dual-modal-imaging-guided chemo-photothermal combination therapy, Adv. Mater. (2015). https://doi.org/10.1002/adma.201405634.

[157] W.Y. Jeong, M.S. Kang, H. Lee, J.H. Lee, J. Kim, D.W. Han, K.S. Kim, Recent trends in photoacoustic imaging techniques for 2d nanomaterial-based phototherapy, Biomedicines. (2021). https://doi.org/10.3390/biomedicines9010080.

[158] H. Ebrahimzade, G.R. Khayati, M. Schaffie, Preparation and kinetic modeling of β-Co(OH)2 nanoplates thermal decomposition obtained from spent Li-ion batteries, Adv. Powder Technol. (2017). https://doi.org/10.1016/j.apt.2017.08.005.

[159] P.S. Gaikar, S.T. Navale, S.L. Gaikwad, A. Al-Osta, V. V. Jadhav, P.R. Arjunwadkar, M. Naushad, R.S. Mane, Pseudocapacitive performance of a solution-processed β-Co(OH)2 electrode monitored through its surface morphology and area, Dalt. Trans. (2017). https://doi.org/10.1039/c6dt04581b.

[160] P. Panigrahi, D. Jini, H. Bae, H. Lee, R. Ahuja, T. Hussain, Two-dimensional Janus monolayers of MoSSe as promising sensor towards selected adulterants compounds, Appl. Surf. Sci. (2021). https://doi.org/10.1016/j.apsusc.2020.148590.

[161] D. Singh, R. Ahuja, Highly sensitive gas sensing material for environmentally toxic gases based on Janus NbSeTe monolayer, Nanomaterials. (2020). https://doi.org/10.3390/nano10122554.

[162] M. Bae, J.K. Oh, S. Liu, N. Nagabandi, Y. Yegin, W. Deflorio, L. Cisneros-Zevallos, E.M.A. Scholar, Nanotoxicity of 2d molybdenum disulfide, mos2, nanosheets on beneficial soil bacteria, bacillus cereus and pseudomonas aeruginosa, Nanomaterials. (2021). https://doi.org/10.3390/nano11061453.

[163] E.L.K. Chng, Z. Sofer, M. Pumera, MoS2 exhibits stronger toxicity with increased exfoliation, Nanoscale. (2014). https://doi.org/10.1039/c4nr04907a.

[164] J. Kaur, M. Singh, C. Dell'Aversana, R. Benedetti, P. Giardina, M. Rossi, M. Valadan, A. Vergara, A. Cutarelli, A.M.I. Montone, L. Altucci, F. Corrado, A. Nebbioso, C. Altucci, Biological interactions of biocompatible and water-dispersed MoS2 nanosheets with bacteria and human cells, Sci. Rep. (2018). https://doi.org/10.1038/s41598-018-34679-y.

Journal Pre-proof

[165] B. Domi, K. Bhorkar, C. Rumbo, L. Sygellou, S.N. Yannopoulos, R. Quesada, J.A. Tamayo-Ramos, Fate assessment of commercial 2D MoS2aqueous dispersions at physicochemical and toxicological level, Nanotechnology. (2020). https://doi.org/10.1088/1361-6528/aba6b3.

[166] Z. Sobańska, L. Zapór, M. Szparaga, M. Stępnik, Biological effects of molybdenum compounds in nanosized forms under in vitro and in vivo conditions, Int. J. Occup. Med. Environ. Health. (2020). https://doi.org/10.13075/ijomeh.1896.01411.

[167] C. Chaves-Lopez, H.N. Nguyen, R.C. Oliveira, E.T. Nadres, A. Paparella, D.F. Rodrigues, A morphological, enzymatic and metabolic approach to elucidate apoptotic-like cell death in fungi exposed to h- and α-molybdenum trioxide nanoparticles, Nanoscale. (2018). https://doi.org/10.1039/c8nr06470a.

[168] N. Desai, S. Mali, Chemically Grown MoO3 Nanorods for Antibacterial Activity Study, J. Nanomed. Nanotechnol. (2015). https://doi.org/10.4172/2157-7439.1000338.

[169] S. Vihodceva, A. Šutka, M. Sihtmäe, M. Rosenberg, M. Otsus, I. Kurvet, K. Smits, L. Bikse, A. Kahru, K. Kasemets, Antibacterial activity of positively and negatively charged hematite (α-fe2 o3) nanoparticles to escherichia coli, staphylococcus aureus and vibrio fischeri, Nanomaterials. (2021). https://doi.org/10.3390/nano11030652.

[170] C. Wang, H. Jia, L. Zhu, H. Zhang, Y. Wang, Toxicity of α-Fe2O3 nanoparticles to Artemia salina cysts and three stages of larvae, Sci. Total Environ. (2017). https://doi.org/10.1016/j.scitotenv.2017.04.183.

[171] M. Ates, I.C.C. Cimen, I. Unal, B. Kutlu, B. Ertit Tastan, D. Danabas, O. Aksu, Z. Arslan, Assessment of impact of α-Fe2O3 and γ-Fe2O3 nanoparticles on phytoplankton species Selenastrum capricornutum and Nannochloropsis oculata, Environ. Toxicol. (2020). https://doi.org/10.1002/tox.22875.

[172] X. Wang, Y. Gu, D. Johnson, C. Chen, Y. Huang, The toxicity and DNA-damage mechanism of α-Fe2O3 nanoparticles, Med. Chem. Res. (2017). https://doi.org/10.1007/s00044-016-1753-1.

[173] C.A. Sousa, H.M.V.M. Soares, E. V. Soares, Toxic effects of nickel oxide (NiO) nanoparticles on the freshwater alga Pseudokirchneriella subcapitata, Aquat. Toxicol. (2018). https://doi.org/10.1016/j.aquatox.2018.08.022.

[174] Z. Sabouri, A. Akbari, H.A. Hosseini, A. Hashemzadeh, M. Darroudi, Bio-based synthesized NiO

Journal Pre-proof

nanoparticles and evaluation of their cellular toxicity and wastewater treatment effects, J. Mol. Struct. (2019). https://doi.org/10.1016/j.molstruc.2019.04.075.

[175] G.A. Shah, J. Ahmed, Z. Iqbal, F. ul Hassan, M.I. Rashid, Toxicity of NiO nanoparticles to soil nutrient availability and herbage N uptake from poultry manure, Sci. Rep. (2021). https://doi.org/10.1038/s41598-021-91080-y.

[176] R.J. Vandebriel, W.H. De Jong, A review of mammalian toxicity of ZnO nanoparticles, Nanotechnol. Sci. Appl. (2012). https://doi.org/10.2147/NSA.S23932.

[177] S. Sruthi, J. Ashtami, P. V. Mohanan, Biomedical application and hidden toxicity of Zinc oxide nanoparticles, Mater. Today Chem. (2018). https://doi.org/10.1016/j.mtchem.2018.09.008.

[178] F. Chen, L. Wu, X. Xiao, L. Rong, M. Li, X. Zou, Mixture toxicity of zinc oxide nanoparticle and chemicals with different mode of action upon Vibrio fischeri, Environ. Sci. Eur. (2020). https://doi.org/10.1186/s12302-020-00320-x.

[179] M. Abudayyak, T.A. Gurkaynak, G. Özhan, In vitro evaluation of cobalt oxide nanoparticle-induced toxicity, Toxicol. Ind. Health. (2017). https://doi.org/10.1177/0748233717706633.

[180] F. Cappellini, Y. Hedberg, S. McCarrick, J. Hedberg, R. Derr, G. Hendriks, I. Odnevall Wallinder, H.L. Karlsson, Mechanistic insight into reactivity and (geno)toxicity of well-characterized nanoparticles of cobalt metal and oxides, Nanotoxicology. (2018). https://doi.org/10.1080/17435390.2018.1470694.

[181] S. Dubey, J. Kumar, A. Kumar, Y.C. Sharma, Facile and green synthesis of highly dispersed cobalt oxide (Co3O4) nano powder: Characterization and screening of its eco-toxicity, Adv. Powder Technol. (2018). https://doi.org/10.1016/j.apt.2018.03.009.

[182] S. Chinde, N. Dumala, M.F. Rahman, S.S.K. Kamal, S.I. Kumari, M. Mahboob, P. Grover, Toxicological assessment of tungsten oxide nanoparticles in rats after acute oral exposure, Environ. Sci. Pollut. Res. (2017). https://doi.org/10.1007/s11356-017-8892-x.

[183] A.L. Popov, N.M. Zholobak, O.I. Balko, O.B. Balko, A.B. Shcherbakov, N.R. Popova, O.S. Ivanova, A.E. Baranchikov, V.K. Ivanov, Photo-induced toxicity of tungsten oxide photochromic nanoparticles, J. Photochem. Photobiol. B Biol. (2018). https://doi.org/10.1016/j.jphotobiol.2017.11.021.

[184] H. Xu, F. Han, C. Xia, S. Wang, R.M. Ramachandran, C. Detavernier, M. Wei, L. Lin, S.

Zhuiykov, Wafer-Scale Fabrication of Sub-10 nm TiO2-Ga2O3 n-p Heterojunctions with Efficient Photocatalytic Activity by Atomic Layer Deposition, Nanoscale Res. Lett. (2019). https://doi.org/10.1186/s11671-019-2991-1.

[185] H.J. Bae, T.H. Yoo, S. Kim, W. Choi, Y.S. Song, D.K. Kwon, B.J. Cho, W.S. Hwang, Enhanced photocatalytic degradation of 2-butanone using hybrid nanostructures of gallium oxide and reduced graphene oxide under ultraviolet-C irradiation, Catalysts. (2019). https://doi.org/10.3390/catal9050449.

[186] A.M. Ramesh, A. Gangadhar, M. Chikkamadaiah, S. Shivanna, Hydrothermal synthesis of Ga_2O_3/TiO2 nanocomposites with highly enhanced solar photocatalysis and their biological interest, J. Photochem. Photobiol. (2021). https://doi.org/10.1016/j.jpap.2021.100020.

[187] T.H. Yoo, H. Ryou, I.G. Lee, J. Cho, B.J. Cho, W.S. Hwang, Comparison of Ga2O3 and TiO2 nanostructures for photocatalytic degradation of volatile organic compounds, Catalysts. (2020). https://doi.org/10.3390/catal10050545.

[188] Z.X. Qiang, Y.L. Hong, A. Tang meng, P.Y. Pu, ZnO, TiO2, SiO2, and Al2O3 Nanoparticlesinduced Toxic Effects on Human Fetal Lung Fibroblasts, Biomed Env. Sci,. (2011).

[189] Y. Dağlıoğlu, B. Yılmaz Öztürk, Effect of concentration and exposure time of ZnO-TiO2 nanocomposite on photosynthetic pigment contents, ROS production ability, and bioaccumulation of freshwater algae (Desmodesmus multivariabilis), Caryologia. (2018). https://doi.org/10.1080/00087114.2017.1400262.

[190] M. Geppert, L. Sigg, K. Schirmer, Toxicity and translocation of Ag, CuO, ZnO and TiO2 nanoparticles upon exposure to fish intestinal epithelial cells, Environ. Sci. Nano. 8 (2021) 2249–2260. https://doi.org/10.1039/D1EN00050K.

Journal Pre-proof

Journal Pre-proof

Highlights:

- 2D materials have an emerging role in biomedical applications in therapeutics and diagnostics
- 2D materials can cause biological and environment toxicity
- Safety studies need to conducted to assess toxicity of 2D materials prior to their human use
- Surfactants can confer better functionality and lesser toxicity to the 2D materials

Journal Pre-proof

Journal Pre-proof

Declaration of interests

☒ The authors declare that they have no known competing financial interests or personal relationships that could have appeared to influence the work reported in this paper.

☐The authors declare the following financial interests/personal relationships which may be considered as potential competing interests:

NA

On behalf of all author

Dr Murtaza Tambuwala

Journal Pre-proof